Provided for non-commercial research and education use.
Not for reproduction, distribution or commercial use.

This article appeared in a journal published by Elsevier. The attached copy is furnished to the author for internal non-commercial research and education use, including for instruction at the authors institution and sharing with colleagues.

Other uses, including reproduction and distribution, or selling or licensing copies, or posting to personal, institutional or third party websites are prohibited.

In most cases authors are permitted to post their version of the article (e.g. in Word or Tex form) to their personal website or institutional repository. Authors requiring further information regarding Elsevier's archiving and manuscript policies are encouraged to visit:

http://www.elsevier.com/copyright

Author's personal copy

Journal of Quantitative Spectroscopy & Radiative Transfer 110 (2009) 573–596

Contents lists available at ScienceDirect

Journal of Quantitative Spectroscopy & Radiative Transfer

journal homepage: www.elsevier.com/locate/jqsrt

IUPAC critical evaluation of the rotational–vibrational spectra of water vapor. Part I—Energy levels and transition wavenumbers for $H_2{}^{17}O$ and $H_2{}^{18}O$

Jonathan Tennyson [a,*], Peter F. Bernath [b], Linda R. Brown [c], Alain Campargue [d], Michel R. Carleer [e], Attila G. Császár [f], Robert R. Gamache [g], Joseph T. Hodges [h], Alain Jenouvrier [i], Olga V. Naumenko [j], Oleg L. Polyansky [a], Laurence S. Rothman [k], Robert A. Toth [c], Ann Carine Vandaele [l], Nikolai F. Zobov [m], Ludovic Daumont [i], Alexander Z. Fazliev [j], Tibor Furtenbacher [f], Iouli E. Gordon [k], Semen N. Mikhailenko [j], Sergei V. Shirin [m]

[a] Department of Physics and Astronomy, University College London, London WC1E 6BT, UK
[b] University of York, York, UK
[c] Jet Propulsion Laboratory, California Institute of Technology, Pasadena, CA, USA
[d] Université Joseph Fourier, Grenoble, France
[e] Université Libre de Bruxelles, Brussels, Belgium
[f] Loránd Eötvös University, Budapest, Hungary
[g] University of Massachussets, Lowell, MA, USA
[h] National Institute of Standards and Technology, Gaithersburg, MD, USA
[i] Université de Reims Champagne-Ardenne, Reims, France
[j] Institute of Atmospheric Optics, Russian Academy of Sciences, Tomsk, Russia
[k] Harvard-Smithsonian Center for Astrophysics, Cambridge, MA, USA
[l] Institut d'Aéronomie Spatiale de Belgique, Brussels, Belgium
[m] Institute of Applied Physics, Russian Academy of Sciences, Nizhny Novgorod, Russia

ARTICLE INFO

Article history:
Received 17 December 2008
Received in revised form
12 February 2009
Accepted 13 February 2009

Keywords:
Water vapor
Transition wavenumbers
Atmospheric physics
Energy levels
MARVEL
Information system
Database
Infrared spectra
Microwave spectra

ABSTRACT

This is the first part of a series of articles reporting critically evaluated rotational–vibrational line positions, transition intensities, pressure dependence and energy levels, with associated critically reviewed assignments and uncertainties, for all the main isotopologues of water. The present article contains energy levels and data for line positions of the singly substituted isotopologues $H_2{}^{17}O$ and $H_2{}^{18}O$. The procedure and code MARVEL, standing for measured active rotational–vibrational energy levels, is used extensively in all stages of determining the validated levels and lines and their self-consistent uncertainties. The spectral regions covered for both isotopologues $H_2{}^{17}O$ and $H_2{}^{18}O$ are $0-17\,125\ cm^{-1}$. The energy levels are checked against ones determined from accurate variational calculations. The number of critically evaluated and recommended levels and lines are, respectively, 2687 and 8614 for $H_2{}^{17}O$, and 4839 and 29 364 for $H_2{}^{18}O$. The extensive lists of MARVEL lines and levels obtained are deposited in the Supplementary Material, as well as in a distributed information system applied to water, W@DIS, where they can easily be retrieved. A distinguishing feature of the present evaluation of water spectroscopic data is the systematic use of all available experimental data and validation by first-principles theoretical calculations.

© 2009 Elsevier Ltd. All rights reserved.

* Corresponding author.
E-mail address: j.tennyson@ucl.ac.uk (J. Tennyson).

0022-4073/$ - see front matter © 2009 Elsevier Ltd. All rights reserved.
doi:10.1016/j.jqsrt.2009.02.014

Author's personal copy

1. Introduction

1.1. General background

The water molecule, containing three nuclei and 10 electrons, is one of the simplest molecules and, at the same time, it is the most abundant polyatomic molecule in the universe. Its electronic structure is rather simple: the ground electronic state of water is very well separated from all the excited states. As a triatomic molecule, water has only three vibrational degrees of freedom. Of the three fundamental vibrations, two can be characterized as stretching vibrations (a symmetric and an antisymmetric one for symmetrically substituted isotopologues), while at about half of the energy of the stretches there is a totally symmetric bending vibration. The water molecule rotates as an asymmetric top and has characteristically small moments of inertia. As far as the nuclear dynamics of the water molecule is concerned, it exhibits several peculiarities. For example, due to the presence of two light hydrogen atoms, its vibrations are of large amplitude, and separation of the vibrational and rotational degrees of freedom is rather poor. As a consequence, the usual perturbational treatments used for interpreting molecular spectra have poor convergence characteristics [1], calling for more sophisticated, variational techniques for the interpretation of the rotational–vibrational spectra of water isotopologues.

The full characterization of the spectrum of water vapor from the microwave to the near ultraviolet is a prerequisite for modeling and understanding of many fields in chemistry, physics and engineering [2]. Topics include (1) atmospheric modeling, with emphasis on the definitive understanding of global warming, as water vapor is responsible for about 70% of the known atmospheric absorption of sunlight and the majority of the greenhouse effect, (2) communication-related fields using the Earth's atmosphere, such as satellites and telecommunication, (3) astrophysics, such as the atmospheres of most cool stars and brown dwarfs where hot water is a major constituent, (4) water lasers and masers, widespread in outer space, (5) study of comets, based on fluorescence spectroscopy, and (6) combustion research, such as rocket exhausts, forest fires, and turbine engines as hot steam is a major product of most combustion processes. Note also that the spectroscopy of species of low abundance in the atmosphere or in outer space is hampered considerably by the omnipresence of water lines in the observed spectra.

Water spectra have been the subject of immense scientific effort resulting in a large quantity of data. They are used mostly without critical evaluation, comparison, and inclusion in annotated databases, an exception being the room temperature (296 K) HITRAN database [3,4].

The primary results of spectroscopic measurements on water, or indeed on any other molecule, are wavenumbers of line centers, line intensities, and parameters describing line profiles. There are several reasons why it is often more convenient to convert the transition wavenumbers to energy levels. First, this process reduces the volume of experimental information considerably. On average about 10 levels could be used to reproduce about 40 lines by the energy difference formula. Second, having a set of experimentally derived energy levels, the wavenumbers of the line centers of spectra in different regions can be restored with practically experimental accuracy. Spectroscopists often do this for the purpose of line assignment of new spectra and call assignment obtained this way a "trivial assignment". This technique has recently been deployed as part of a stable spectral line fitting algorithm [5]. Third, theoretical models produce energy levels first and other, secondary programs are usually used to produce the line wavenumbers and line intensities. Thus, it is simpler and more natural to compare the calculated and the experimentally derived energy levels, whereby no use of secondary programs is required. Finally, energy-level lists such as those presented here provide an excellent starting point for the computation of partition functions and related thermodynamic and thermochemical properties [6].

1.2. Establishment of the task group and organization of the project

The present IUPAC-sponsored collaborative effort (see Table 1 for members of the Task Group and their individual tasks) is aimed at devising and constructing a database comprising, eventually, the complete linelist for water for both reference purposes and for subsequent studies utilizing this information at all temperatures. The linelist to be compiled will include annotated theoretical and (where available) experimental/empirical values of transition wavenumbers, intensities, and pressure broadening parameters for all major isotopologues of water ($H_2{}^{16}O$, $H_2{}^{17}O$, $H_2{}^{18}O$, $HD^{16}O$, $HD^{17}O$, $HD^{18}O$, $D_2{}^{16}O$, and $D_2{}^{17}O$. The database will be comprised three parts: (a) energy levels and hence transition wavenumbers; (b) transition intensities; and (c) line-profile parameters. This paper, the first in a series of planned reports, presents experimentally determined transitions and related energy levels, with associated uncertainties, for the $H_2{}^{17}O$ and $H_2{}^{18}O$ monosubstituted isotopologues of water.

Probably the first attempt at a compilation of water transition data was by Gates et al. [7]. A more comprehensive compilation of line parameters of water vapor, between 0 and 4350 cm^{-1}, for $H_2{}^{16}O$, $H_2{}^{17}O$, and $H_2{}^{18}O$, was assembled by Flaud et al. [8]. A significant previous attempt at a comprehensive evaluation of empirical energy levels for the main isotopologue of water, $H_2{}^{16}O$, was performed by Tennyson et al. [9]. Recently, some of us [10–12] have developed a robust procedure called MARVEL, standing for measured active rotational–vibrational energy levels, for inverting experimental transition data to give energy levels and associated uncertainties. The MARVEL procedure has been used extensively during the course of the work of the Task Group. This procedure is described in Section 2 and applied in subsequent sections. The water line positions and energy level data resulting from the efforts of the Task Group, mostly presented as

Author's personal copy

Table 1
Members of the Task Group.

Name	Tasks[a]
Jonathan Tennyson (Chair), University College London, London, United Kingdom	TCHV
Peter Bernath University of York, York, United Kingdom	ECH
Alain Campargue, Université Joseph Fourier, Grenoble, France	ECH
Michel R. Carleer, Université Libre de Bruxelles, Brussels, Belgium	ECH
Attila G. Császár, Eötvös University, Budapest, Hungary	TDV
Robert Gamache, University of Massachussets, Lowell, MA, USA	TL
Joseph T. Hodges, National Institute of Standards, and Technology, Gaithersburg, MD, USA	ESVL
Alain Jenouvrier[b], University of Reims, Reims, France	EC
Olga Naumenko, Russian Academy of Sciences, Tomsk, Russia	TCH
Oleg Polyansky, University College London, London, United Kingdom	TCHD
Laurence S. Rothman, Harvard-Smithsonian Center, for Astrophysics, Cambridge, MA, USA	DVL
Robert A. Toth, California Institute of Technology, Pasadena, CA, USA	EC
Ann Carine Vandaele, Institut d'Aéronomie Spatiale de Belgique, Brussels, Belgium	EC
Nikolai Zobov, Russian Academy of Sciences, Nizhny Novgorod, Russia	TCH

[a] Field of expertise of the individual as related to the IUPAC project, whereby E: experimentalist, T: theoretician, C: cold water spectra, H: hot water spectra, D: data handling, V: data validation, S: standardization, and L: line profiles.
[b] From September 2007 replaced by Ludovic Daumont.

Supplementary Material to this article, have also been deposited in the distributed information system applied to water, W@DIS [13,14].

A distinguishingfeature of the present study is the joint utilization of all available experimental and the best theoretical transition and energy level data. The long-term aim of such an undertaking is the establishment of the complete linelist for all water isotopologues. While determination of a complete linelist is outside the scope of present-day experiments, it can be determined by means of sophisticated first-principles computations. Consequently, as long as experiments have a higher precision than even the most advanced computations that can be performed for water, the complete linelist will necessarily contain accurate experimental data and less accurate computational data. MARVEL-type efforts help to replace as many computed lines as possible with their experimental counterparts. This method also, as has been demonstrated [12], helps to reduce the uncertainty with which a transition has been determined.

2. Methodology

The methods employed in this study for collecting and critically evaluating experimental transition wavenumbers and uncertainties and for inverting the wavenumbers in order to obtain the best possible energy levels with uncertainties are based on the MARVEL procedure recently developed by Furtenbacher et al. [10]. MARVEL is built on the X-matrix method of Flaud et al. [15], the Active Thermochemical Tables (ATcT) approach of Ruscic and co-workers [16], and an iterative robust reweighting scheme advocated by Watson [17], and it simultaneously processes *all* the available assigned experimental lines and the associated energy levels for the chosen isotopologue of the molecule under consideration. While the resulting energy levels could be called empirical, in order to emphasize the process they were derived from, the evaluated and validated energy levels will be called MARVEL energy levels throughout this study.

In order to help critical evaluation and tracking of the transitions and energy levels even after a prolonged time, the dataset compiled must also contain information about the sources of the measured transitions. Therefore, besides the obvious attributions of the data, listed under 'Physical conditions' in Tables 2 and 3 and in related 'Comments' in Sections 3.3 and 3.4, the same tables give each data source a tag based on year of publication and the names of the authors. This tag will be used throughout our series of papers, in the transition lists that form the MARVEL inputs, and are used in W@DIS, standing for water data in a distributed information system (see Section 2.4 for details), to provide a unique identifier of the

Author's personal copy

Table 2
Data sources and their characteristics for $H_2{}^{17}O$.[a] See Section 3.3 for comments.

Tag	Range	Trans.	Physical conditions					Comments
	(cm^{-1})	A/V	T (K)	p (hPa)	Abun. (%)	Rec.	L (m)	
71StBe [21]	0.45, 6.47	2/2				MW		(2a)
75DeHe [27]	0–18	7/7			30	MW	1	(2b)
99MaNaNaOd [50]	16–173	127/127		⩽0.1	10		0.5	(2c)
81Partridg [38]	16–47	17/17		1.3–21.3	10		0.8–13	(2d)
78KaKaKy [33]	30–720	20/18	RT	0.7–5.3	Nat	FTS	1	(2e)
80KaKy [35]	54–728	373/371		0.7–5.6	24	FTS	0.7	(2f)
77Winther [28]	61–392	48/43	295	0.7–23.7	Nat	FTS	3	(2g)
98Toth [49]	599–797	31/31	RT	⩽37.9	Nat	FTS	0.25–433	
92Toth [44]	1012–2224	699/698	297	0.3–6.9	⩽59.9	FTS	2.39	
93Totha [45]	1314–3945	336/336	296	0.4–18.4	⩽59.9	FTS	2.39–433	
83Guelachv [42]	1316–1986	197/197	RT	2.0	Nat	FTS	16–44.17	(2h)
71WiNaJo [22]	1338–1913	133/111	–	–	–	LS	–	(2i)
78JoMc [34]	1613–1644	2/1	RT	0.0066	11	SS		(2j)
94Totha [46]	3163–4298	824/824	296	0.4–18.4	⩽57.7	FTS	2.39–433	(2k)
69FrNaJo [19]	3445–3942	103/94	RT		$H_2{}^{18}O$ Enr	GS	1	(2l)
73CaFlGuAm [25]	3582–3909	58/56	RT	1.3	Nat	FTS	8	(2m)
83PiCoCaFl [41]	3649, 3830	2/2	1200	2.59	Nat	LS	1.3	(2n)
02MiTyStAl [53]	4206–4999	8/8						
07JeDaReTy [67]	4206–6600	574/572	RT	1.4-22.7	Nat	FTS	0.3–1804	(2o)
05Tothb [59]	5018–5685	312/312	296	⩽19.9	⩽60	FTS	1.5–433	
77ToFlCaa [29]	5174–5525	84/71	296	3.1	0.1	GS	8–48	(2p)
07MiLeKaCa [68]	5988–7016	235/235	RT	10–20	Nat	CW-CRDS	NR	
04MaRoMiNa [57]	6171–6747	183/181	RT	1.5–20	Nat	CW-CRDS	NR	(2q)
94Tothb [47]	6617–7639	854/849	296–298	1.4–19.2	⩽59.5	FTS	2.39–433	(2r)
77ToFlCab [30]	7094–7333	20/14	RT		0.1	GS		(2s)
05ToTe [60]	7424–9052	183/178	294.4	20.1	Nat	FTS	480.8	(2t)
06LiHuCaMa [64]	8564–9332	429/429	297	2.1–13.1	5	FTS	15–105	(2u)
99CaFlMaBy [51]	9711–10 883	1063/1058	RT		Enr	FTS		(2v)
05ToNaZoSh [63]	10 807–13 893	246/240						
05TaNaBrTe [61]	11 365–14 472	773/761	RT		Enr	FTS	434	(2w)
07MaToCa [66]	11 547–12 729	310/297	RT			ICLAS	4800–14 400	(2x)
06NaSnTaSh [65]	16 666–17 125	513/474	294	25	80 ± 5	CRDS	NR	(2y)

[a] As explained at the beginning of Section 2, the tags listed are used to identify experimental data sources throughout this paper. The range given represents the range corresponding to wavenumber entries within the MARVEL input file of the particular water isotopologue and not the range covered by the relevant experiment. Uncertainties of the individual lines can be obtained from the Supplementary Material. Trans.: transitions, with A: number of assigned transitions in the original paper, V: number of transitions validated in this study. T: temperature (K), given explicitly when available from the original publication, with RT: room temperature. p: pressure (hPa). Abun.: abundance (%) of the given isotopologue in the gas mixture, with Enr: enriched and Nat: natural abundance. Rec.: experimental technique used for the recording of the spectrum, with MW: microwave spectroscopy, GS: grating spectrograph, LS: laser spectroscopy, SS: Stark spectroscopy, FTS: Fourier-transform spectroscopy, ICLAS: intracavity laser absorption spectroscopy, CRDS: cavity ringdown spectroscopy, CW-CRDS: continuous wave cavity ringdown spectroscopy. L: pathlength (m), with NR: not relevant.

primary data sources. Within MARVEL, each transition has an individual label, involving this tag and the sequence number of the transition in the original publication.

In practice, the transitions collected and remaining in the database after critical evaluation are split into spectroscopic networks (SNs). SNs contain all interconnecting rotational–vibrational energy levels supported by the grand database of the transitions. This, for example, means that transitions involving "*ortho*" or "*para*" states of both $H_2{}^{17}O$ and $H_2{}^{18}O$ are treated separately. The simple explanation behind distinct SNs is that the spins of the protons can couple to produce states with $I = 0$ (*para*) and $I = 1$ (*ortho*). In a field-free environment each rotational–vibrational state is associated with only one nuclear spin state; we neglect the possibility of interchange since *ortho–para* transitions are predicted to be extremely weak [18] and have yet to be observed. In the high-temperature limit (above 50 K), 75% of the molecules are in *ortho* and 25% are in *para* states.

During the course of this work, there was a special effort to validate both the experimental transition wavenumbers and the derived energy levels. This involved several steps, detailed in the next subsections. The validation process involved not only MARVEL and pre- and post-processing, but also energy-level computations based on empirical potential energy hypersurfaces and the rigorous (exact) quantum labels these computations provide for the levels.

2.1. From transitions to energy levels

In the present work the following steps were followed to go from measured and assigned transitions to MARVEL energy levels. First, all experimental and high-quality computational data were gathered for the isotopologues $H_2{}^{17}O$ [10,12,19–70] and $H_2{}^{18}O$ [12,19,21–26,28–38,40–47,49,50,52–58,60–64,66–110].

Author's personal copy

Table 3
Data sources and their characteristics for $H_2{}^{18}O$.[a] See Section 3.4 for comments.

Tag	Range	Trans.	Physical conditions					Comments
	(cm^{-1})	A/V	T (K)	p (hPa)	Abun. (%)	Rec.	L (m)	
70PoJo [73]	0.19	1/1						
71StBe [21]	0.19, 6.78	2/2				MW		
72DeHeCoGo [23]	6.78–24.86	11/11	RT		Nat	MW		
06GoMaGuKn [107]	6.79–18.27	6/6	RT	0.0007–0.0013	Nat	LDS		(3a)
87BeKoPoTr [88]	15.58–21.59	9/9	RT	0.4–0.8	20			(3b)
76FlGi [76]	13–40	12/11	RT		90		0.2	(3c)
99MaNaNaOd [50]	18.5–174.8	118/118		$\leqslant 10^{-3}$	96	MW	0.5	(3d)
81Partridg [38]	21.6–46.8	16/16	RT	1.3–13	16		0.8–13	
85Johns [82]	33.2–280.3	146/146		$\leqslant$2.6	Nat	FTS	0.15	
80KaKy [35]	53.6–725.1	370/369	RT	1.1–5.6	29	FTS	1–3	(3e)
77Winther [28]	54.5–524.1	122/105	296	0.7–23.7	Nat	FTS	3	(3f)
78KaKaKy [33]	55.2–370.5	62/61	RT	$\leqslant$5.33	Nat	FTS	1	(3g)
69BePoTo [72]	178–398	10/5						(3h)
03MiTyMe [104]	399–806	143/167	1370	16	Nat	FTS	NR	(3i)
98Toth [49]	596–944	75/75	296–302	$\leqslant$38	Nat	FTS	0.25–433	
92Toth [44]	1010–2219	779/776	297	0.3–6.9	$\leqslant$98.1	FTS	2.39	(3j)
83Guelachv [42]	1268–2053	306/306	297–299	$\leqslant$2	Nat	FTS	16–44.17	(3k)
93Totha [45]	1312–1934 2893–3879	461/460	296	$\leqslant$18.4	$\leqslant$98.1	FTS	2.39–433	
71WiNaJo [22]	1332–1955	234/191				LS		(3m)
06JoPaZeCo [109]	1483.9, 1485.0	2/2	293	4–14	Enr	LS	0.2&9.6	
78JoMc [34]	1640.2, 1693.7	2/2		0.0066	11	LDS	0.2	(3n)
75ToMa [75]	2900–3400	335/302	RT	2.6–10.0	50	GS	8–40	(3o)
94Totha [46]	3117–4340	1038/1032	RT	$\leqslant$18.4	$\leqslant$94.0	FTS	2.39–433	(3p)
69FrNaJo [19]	3347–4029	618/529			Enr	GS	1	(3q)
83PiCoCaFl [41]	3447–3890	49/47	1200	1.0&2.6	Nat	LS	1.3	(3r)
73CaFlGuAm [25]	3534–3936	128/128	RT	1.3	Nat	FTS	8	(3s)
83ToBr [81]	3718–3738	3/3	RT			FTS		(3t)
02MiTyStAl [53]	4200–4997	70/70						
07JeDaReTy [67]	4201–6599	1059/1054	RT	1.4–22.7	Nat	FTS	0.3–1804	(3u)
85ChMaFlCa [83]	4433–6087	1367/1360	300		73			(3v)
86ChMaFlCa [84]	4897–5918	186/186	300 ± 0.5	3.68	73		49, 217	(3w)
77ToFlCaa [29]	5036–5638	527/492	296	3.0	50	GS	8–48	(3x)
06LiDuSoWa [108]	1082–5997	5220/5205	RT	$\leqslant$13.07	95	FTS	15, 105	(3y)
07MiLeKaCa[68]	5918–7015	447/447	RT	1.5–20	Nat	CW-CRDS	NR	
86ChMaCaFlb [85]	5924–7862	2137/2105			73			(3z)
06LiNaSoVo [106]	6001–8003	3179/3148	297	$\leqslant$13.07	75	FTS	15, 105	(3aa)
04MaRoMiNa [57]	6134–6748	442/419	RT	22.3	Nat	CW-CRDS		(3bb)
94Tothb [47]	6608–7639	966/959	296–298	$\leqslant$18.8	$\leqslant$31.4	FTS	2.39–433	(3cc)
77ToFlCab [30]	6975–7387	323/321	RT	3.0	50	GS	24	(3dd)
01MoSaGiCi [102]	7182–7184	3/3						
05ToTe [60]	7428–9271	505/486	294	20.08	Nat	FTS		(3ee)
06LiHuCaMa [64]	8012–9337	1533/1528	RT	2.2–13.1	Several	FTS	$\leqslant$105	(3ff)
05ToNaZoSh [63]	9251–14 385	733/706						
87ChMaFlCa [87]	9640–11 374	2092/2087	300	3.6–6,3	73	FTS	49–434	(3gg)
07MaToCa [66]	11 520–12 810	1891/1843	RT	1.3–26	55	ICLAS	4800–14 400	(3hh)
95ByNaPeSc [98]	11 600–12 696	736/730	RT		73	FTS	434	(3ii)
05TaNaBrTe [61]	12 403–14 518	1085/1070	RT	3.6	73	FTS	434	(3jj)
04TaSnUbTe [105]	16 577–17 121	367/264	RT	24	Enr	CRDS	NR	(3kk)

[a] See footnote a to Table 2. LDS, Lamb-dip spectroscopy.

Our strict criterion for the inclusion of experimental data for the present analysis was that only published primary transition data were considered. In this context primary means that no secondary sources, for example ''experimental'' energy levels or transitions based even on accurate model Hamiltonians, have been considered. Tables 2 and 3 list the experimental sources of transition data identified from the above lists for $H_2{}^{17}O$ and $H_2{}^{18}O$, respectively. In order to be used in MARVEL, each transition has to have an initial nonzero uncertainty. In most cases these transitions can be taken directly from the measurements. Note that the ''active'' [16] in the MARVEL acronym is there because the results can easily be updated should further or revised experimental data become available, since this involves simply adding extra lines to the transition files presented as supplementary data to this work and re-running the MARVEL procedure.

The second step involved cleaning the data. A test facility was developed to check all transitions for uniqueness, including uniqueness of the assignment, to avoid duplicating the same datum, and for consistency. The following tests have been performed: (a) for two transitions having the exact same entries, including assignment, wavenumbers, and

Author's personal copy

uncertainties, it is checked whether they are from the same reference (a clear case of a duplicate) or from different references, in which case a warning is issued; (b) if two transitions have the same assignment, it is checked whether their wavenumbers differ by more than a certain cutoff value; if so, a warning is issued; (c) if the difference between two transitions is smaller than a prescribed value and they have distinct assignments, a warning is issued; (d) forbidden assignments, mixing the *ortho* and *para* levels, are searched for; and finally, (e) through a single "inversion and regeneration of the transitions" step, it is checked whether an experimental datum from a given source is compatible with the other assigned line frequencies. Any conflicts arising from the transcription of data were identified and corrected, if possible. Next, the remaining transitions were compared to variational linelists computed using exact rotational–vibrational kinetic energy operators and accurate empirical potential energy surfaces (PESs). The mass-dependent empirically adjusted PESs employed are based on the high-quality, so-called CVRQD ab initio PESs [111,112] of water as fitted to spectroscopic data for $H_2{}^{16}O$, $H_2{}^{17}O$, and $H_2{}^{18}O$ in Ref. [70]. The average precision of the computed rovibrational transitions using these PESs is better than 0.05 cm^{-1}; therefore, experimental transitions which deviated more than 0.5 cm^{-1} from entries in the variational linelists with matching rotational quantum number J and parity, were deleted from the database intended for processing by MARVEL. Finally, transitions which did not obey combination difference rules with a precision better than 0.025 cm^{-1} were removed from the database. In general these transitions are superceded by more accurate, more recent measurements.

The third step involved the actual execution of the MARVEL process. At this stage the uncertainties of the lines were adjusted until a consistent set of experimental uncertainties was obtained. MARVEL uses the robust reweighting algorithm [17] for this step. For details of the reweighted inversion process, see Refs. [10,12]. Uncertainties reported below are given by Eq. (5) of Ref. [10] and correspond to 95% confidence limits which are therefore 2σ.

The procedure employed ensures that the transitions determined with a small uncertainty have a much larger effect on the energy level determination than those transitions that have a much larger uncertainty. There are a number of possible issues with this protocol. Firstly, the measured transition wavenumbers are sensitive to the pressure under which the experiment is performed. For this reason, spectra recorded in pure water vapor are favored where possible (this becomes an important issue for the $H_2{}^{16}O$ spectra not considered here). Secondly, frequency calibration in each particular experiment can be an issue, as this has the potential to lead to systematic shifts in the reported transitions, see Refs. [113,114] for examples. Thirdly, all previous studies using MARVEL [10,12] were based on the exclusive use of room-temperature experiments. Hot spectra are usually considerably richer in transitions but have significantly larger uncertainties and a higher chance for mislabeling. In this work some hot spectra for $H_2{}^{18}O$ were included [41,104] and temperature is made in the data tabulations given in Tables 2 and 3. Fourthly, in the microwave region hyperfine effects may result in measurable splittings of some of the rotational lines. The number of such measurements is very limited and in higher-energy regions the resolution is not sufficient to resolve such fine details. Therefore, such measurements were not considered explicitly. These transitions have been properly averaged in later papers and only the average has been included in the MARVEL treatment, the hyperfine splittings are only mentioned in the appropriate footnotes to Tables 2 and 3. Fifthly, in a few cases, detailed in Sections 3.3 and 3.4, degenerate transitions were added, with appropriate labels, to the transitions file although they were not listed explicitly in the original publication. Such added transitions inherited the tag information of their degenerate pair but are distinguished from them by a capital D at the end of the tag information. These added transitions should prove especially useful during the analysis of hot spectra.

The final step in the procedure was to check the MARVEL energy levels against variational nuclear motion computations. To do this we used spectroscopically determined potential energy hypersurfaces [70] and well-converged variational energy levels were determined by using the program suite DVR3D [116]. This step is of particular importance for levels determined by a single transition or for those levels that form a series of levels interconnected by single transitions known as a branch [117]. Any MARVEL level obtained as part of this work which differed by more than 0.1 cm^{-1} from its variational counterpart was subject to further scrutiny. Those transitions which involved a MARVEL energy level which did not have a matching variational pair, within 0.5 cm^{-1}, were deleted from the MARVEL input and the MARVEL process was repeated until all MARVEL levels had variational counterparts. At the same time the transitions were checked for consistency as the difference between observed and calculated levels generally shows great regularity as J varies for a given vibrational state and value of K_a. Variations of more than $\pm$0.05 cm^{-1} were used to pinpoint inaccurate transition frequencies. The appropriate comments in Sections 3.3 and 3.4 list the transitions removed at this stage. Other levels, which we consider to be marginally reliable, were retained but are flagged in the appropriate entry of the Supplementary Material.

In order to highlight the utility of the variational linelist, Fig. 1 plots the difference between our whole MARVEL energy level datasets (see below) with the corresponding levels computed variationally. For $H_2{}^{17}O$, even the largest deviations are less than 0.15 cm^{-1} as the transitions observed only probe lower K_a levels. For $H_2{}^{18}O$, we find that 87.5% of the observed transitions lie within 0.05 cm^{-1} of their variationally computed counterparts. The largest deviations, obs − calc values of +0.3 cm^{-1}, occur for levels with $J \geqslant 7$ and can be associated with states for which K_a is close to J.

2.2. Labeling

It is a strict requirement that the dataset contains a single unique assignment to label both the lower and the upper states involved in the transitions. Without this information the MARVEL inversion process from transitions to energies cannot be executed.

Author's personal copy

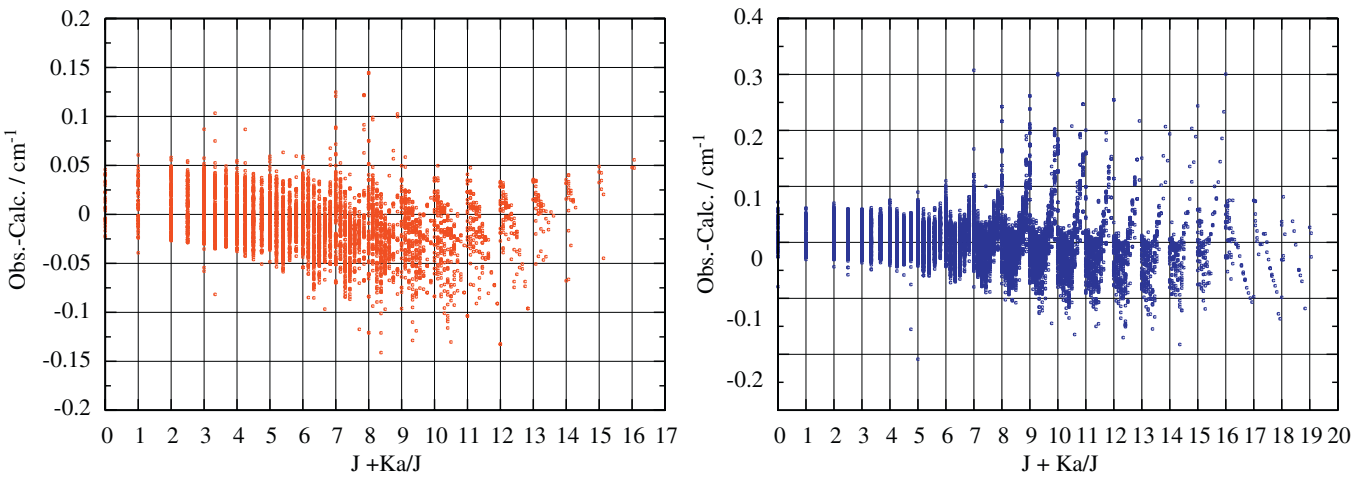

Fig. 1. Differences between "observed" (MARVEL) energy levels and calculated ones from the variational calculations of Shirin et al. [70] for $H_2{}^{17}O$ (left) and $H_2{}^{18}O$ (right).

A useful choice for the labeling of the levels is provided by the usual quantum numbers used by spectroscopists, the standard normal coordinate labeling $(v_1v_2v_3)$ in the case of the vibrations of water. In this notation v_1, v_2, and v_3 stand for the symmetric stretching, bending, and antisymmetric stretching quantum numbers, respectively. The harmonic wavenumbers, ω_i, of the vibrational fundamentals of $H_2{}^{16}O$ are such that $\omega_1 \approx 2\omega_2 \approx \omega_3$. We use the standard asymmetric top quantum numbers JK_aK_c to label the rotational states. Thus, the rotation–vibration levels of each isotopologue are identified uniquely by six labels altogether. For asymmetric top rotational energy, the notation J_τ is sometimes used. This is actually not a different notation since τ is simply given by $K_a - K_c$. It holds, furthermore, that $0 \leqslant [K_a, K_c] \leqslant J$ and $K_a + K_c = J$ or $J+1$.

It should be noted that all of the labels except J described above are only approximate ones and methods to identify the most appropriate labels for higher-energy states of water are still a matter of active research [118]. Rigorous labels, if the hyperfine coupling associated with the nuclear spins is neglected, are the total rotational angular momentum, J, and the total parity, p. There is an additional quantum number specifying *ortho* and *para* states, provided the very weak coupling [18] between such states is neglected. The number $q = (K_a + K_c + v_3)$ is even for *para* states and odd for *ortho* ones. It is possible to add one more number, N, to completely specify each energy level. N is simply the position of a given level in the energy stack for a given combination of J, p and q. This labeling is a natural one for energy levels obtained from variational computations but of only limited usefulness when analysing experimental data since these rarely give a complete set of levels. MARVEL was used to check whether energies with the same rigorous quantum number (J, p and q) but different approximate quantum numbers actually have different energies.

Besides normal modes, other possible approximate vibrational quantum number schemes include the local mode labels [119]. Indeed, these labels are known [120] to give a much more physical description of most of the vibrational levels of $H_2{}^{16}O$ for states in which $v_1 + v_3 \geqslant 4$. The local mode labels are $(n,m)^{\pm}v_2$, where v_2 is the bending quantum number, as in the normal mode picture. For the stretching quantum numbers $n + m = v_1 + v_3$ and the superscripted sign indicates whether the quanta in each local mode appear as a symmetric or antisymmetric combination. Note that when $n = m$, only the symmetric combination is allowed and the superscripted sign is usually omitted. It is more convenient in a database to use normal mode labels, but in practice we choose these labels so that the mapping described above gives the correct local mode energy pattern (see [120] for a discussion of this). In Tables 4 and 5, both the normal and the local mode sets of labels are used.

Finally, we note that for $H_2{}^{16}O$, $H_2{}^{17}O$, and $H_2{}^{18}O$ the vibrational bands form polyads. A polyad number, which we denoted P, can be defined by

$$P = 2v_1 + v_2 + 2v_3, \tag{1}$$

since a quantum of v_1 approximately equals a quantum of v_3 and both are given by about $2v_2$. This polyad quantum number, which is in the form standard for other molecules with polyad structures, is used to label the Vibrational Band Origins (VBOs) of $H_2{}^{17}O$ and $H_2{}^{18}O$ in Tables 4 and 5. The standard notation for the polyads in water, however, is given by defining an alternative polyad number n. For even values of P, n is simply half of P, while for P odd n is half of $P-1$. The polyads are then labeled nv for P even and $nv + \delta$ for P odd. Thus, for example, the polyads $3v$ and $3v + \delta$ correspond to $P = 6$ and 7, respectively. Each polyad contains $(n+1)(n+2)/2$ vibrational states, although there is some evidence from our results that, as n increases, states with significant bending excitation begin to drop off the bottom of the polyad and can even join the polyad below.

It is clear that a relatively good model must be available prior to using MARVEL in order to give proper and unique labels for the experimental transitions. Approximate Hamiltonians as well as variational computations based on highly accurate PESs, obtained perhaps *ab initio* [111,112,121,122], are able to provide these labels for most small molecules of interest and

Author's personal copy

Table 4
MARVEL vibrational band origins (VBO), with polyad number ($P = 2v_1 + v_2 + 2v_3$), normal-mode ($v_1v_2v_3$) and local-mode ($(mn)^{\pm}v_2$) assignments, MARVEL uncertainties (Unc.), and the number of rotational levels (RL) the vibrational levels are holding within the present database, for $H_2{}^{17}O$.[a]

P	$v_1v_2v_3$	$(mn)^{\pm}v_2$	VBO/cm^{-1}	Unc.	RL
0	000	$(00)^{+}0$	0.000000[b]	0	192
1	010	$(00)^{+}1$	1591.325698	51	153
2	020	$(00)^{+}2$	3144.980503	44	78
2	100	$(10)^{+}0$	3653.142275	31	108
2	001	$(10)^{-}0$	3748.318112	31	141
3	030	$(00)^{+}3$	[4657.12]		23
3	110	$(10)^{+}1$	5227.705615	511	69
3	011	$(10)^{-}1$	5320.251634	532	147
4	040	$(00)^{+}4$	[6121.55]		21
4	120	$(10)^{+}2$	6764.725615	511	63
4	021	$(10)^{-}2$	6857.272483	44	94
4	200	$(20)^{+}0$	7193.246415	51	81
4	101	$(20)^{-}0$	7238.714014	54	110
4	002	$(11)^{+}0$	7431.076115	511	27
5	050	$(00)^{+}5$	[7527.50]		1
5	130	$(10)^{+}3$	[8260.80]		3
5	031	$(10)^{-}3$	[8356.53]		18
5	210	$(20)^{+}1$	[8749.85]		34
5	111	$(20)^{-}1$	8792.544010	374	108
6	060	$(00)^{+}6$	[8853.50]		1
5	012	$(11)^{+}1$	8982.869215	511	55
6	*140*	*$(10)^{+}4$*	[*9708.58*]		
6	041	$(10)^{-}4$	[9813.34]		13
7	*070*	*$(00)^{+}7$*	[*10 068.20*]		
6	220	$(20)^{+}2$	[10 269.62]		12
6	121	$(20)^{-}2$	10 311.201765	438	75
6	022	$(11)^{+}2$	[10 501.35]		1
6	300	$(30)^{+}0$	[10 586.06]		62
6	201	$(30)^{-}0$	10 598.475620	517	103
6	102	$(21)^{+}0$	10 853.505315	511	69
6	003	$(21)^{-}0$	11 011.882910	2587	84
7	*150*	*$(10)^{+}5$*	[*11 080.53*]		
7	*051*	*$(10)^{-}5$*	[*11 219.80*]		
8	*080*	*$(00)^{+}8$*	[*11 232.31*]		
7	230	$(20)^{+}3$	[11 749.99]		3
7	131	$(20)^{-}3$	11 792.822208	513	40
7	*032*	*$(11)^{+}3$*	[*11984.35*]		
7	310	$(30)^{+}1$	[12 122.16]		34
7	211	$(30)^{-}1$	12 132.992610	517	94
8	*160*	*$(10)^{+}6$*	[*12 357.87*]		
7	112	$(21)^{+}1$	[12 389.06]		30
9	*090*	*$(00)^{+}9$*	[*12 509.43*]		
7	013	$(21)^{-}1$	12 541.227060	480	51
8	*061*	*$(10)^{-}6$*	[*12 560.95*]		
8	*240*	*$(20)^{+}4$*	[*13 185.20*]		
8	141	$(20)^{-}4$	[13 233.16]		1
8	042	$(11)^{+}4$	[13 427.15]		1
8	320	$(30)^{+}2$	[13 620.56]		3
8	221	$(30)^{-}2$	13 631.499810	569	52
9	071	$(10)^{-}7$	13 808.273310	517	2
8	400	$(40)^{+}0$	[13 809.74]		29
8	301	$(40)^{-}0$	13 812.158110	517	74
8	*122*	*$(21)^{+}2$*	[*13 889.43*]		
8	*023*	*$(21)^{-}2$*	[*14 039.34*]		
8	202	$(31)^{+}0$	[14 203.54]		14
8	103	$(31)^{-}0$	14 296.279510	207	36
8	*004*	*$(22)^{+}0$*	[*14 511.35*]		
10	081	$(10)^{-}8$	[14 954.46]		1
10	260	$(20)^{+}6$	[15 846.11]		2
10	161	$(20)^{-}6$	[15 941.23]		1
10	340	$(30)^{+}4$	[16 509.33]		14
10	241	$(30)^{-}4$	[16 520.03]		8
10	142	$(21)^{+}4$	[16 769.58]		12
10	321	$(40)^{-}2$	16 797.167510	4140	70
10	420	$(40)^{+}2$	[16 798.86]		59

Author's personal copy

Table 4 (*continued*)

P	$v_1v_2v_3$	$(mn)^{\pm}v_2$	VBO/cm^{-1}	Unc.	RL
10	500	$(50)^{+}0$	[16 875.24]		46
10	401	$(50)^{-}0$	16 875.620510	4140	55
10	043	$(21)^{-}4$	[16 934.70]		5
10	222	$(31)^{+}2$	[17 199.89]		1
10	123	$(31)^{-}2$	[17 284.08]		2
10	302	$(41)^{+}0$	[17 436.29]		2

[a] The uncertainties (Unc.) are given in units of 10^{-6} cm^{-1}. For VBOs not determined by the available experimental data, approximate variationally computed VBOs, based on an exact kinetic energy operator and the PES of 08ShZoOvPo [70], are given in brackets. These values should only be used for guidance about the VBOs and should not be taken literally, though their accuracy is expected to be considerably better than 0.1 cm^{-1}. For obvious reason, no Unc's are given for these VBOs. For completeness, the VBOs up to $P = 8$, for which no rovibrational states have been observed are also given. These levels, for which no RL values are given, are printed in italics and correspond to variationally computed values, as well. The VBOs are ordered according to their energies.

[b] The value of the vibrational ground state was fixed to zero with zero uncertainty.

Table 5

MARVEL vibrational band origins (VBO), with polyad number ($P = 2v_1 + v_2 + 2v_3$), normal-mode ($v_1v_2v_3$) and local-mode ($(mn)^{\pm}v_2$) assignments, MARVEL uncertainties, and the number of rotational levels (RL) the vibrational levels are holding within the present database, for $H_2{}^{18}O$.[a]

P	$v_1v_2v_3$	$(mn)^{\pm}v_2$	VBO/cm^{-1}	Unc.	RL
0	000	$(00)^{+}0$	0.000000	0	296
1	010	$(00)^{+}1$	1588.275946	33	227
2	020	$(00)^{+}2$	3139.050001	37	146
2	100	$(10)^{+}0$	3649.685416	51	192
2	001	$(10)^{-}0$	3741.566775	46	216
3	030	$(00)^{+}3$	4648.477803	347	114
3	110	$(10)^{+}1$	5221.243307	386	146
3	011	$(10)^{-}1$	5310.461347	318	207
4	040	$(00)^{+}4$	[6110.43]		80
4	120	$(10)^{+}2$	6755.510207	353	126
4	021	$(10)^{-}2$	6844.598736	222	146
4	200	$(20)^{+}0$	7185.878096	518	151
4	101	$(20)^{-}0$	7228.883335	516	179
4	002	$(11)^{+}0$	7418.724061	301	143
5	050	$(00)^{+}5$	[7514.21]		4
5	130	$(10)^{+}3$	8249.035658	515	76
5	031	$(10)^{-}3$	8341.107933	430	116
5	210	$(20)^{+}1$	8739.525858	515	84
5	111	$(20)^{-}1$	8779.719520	392	143
6	060	$(00)^{+}6$	[8838.62]		1
5	012	$(11)^{+}1$	8967.565058	515	87
6	140	$(10)^{+}4$	[9694.63]		1
6	041	$(10)^{-}4$	9795.331502	486	72
7	070	$(00)^{+}7$	[10 052.17]		10
6	220	$(20)^{+}2$	10 256.584858	515	61
6	121	$(20)^{-}2$	10 295.634509	463	108
6	022	$(11)^{+}2$	10 483.221458	515	53
6	300	$(30)^{+}0$	10 573.916858	515	97
6	201	$(30)^{-}0$	10 585.285194	522	133
6	102	$(21)^{+}0$	10 839.955723	511	90
6	003	$(21)^{-}0$	10 993.681009	463	103
7	150	$(10)^{+}5$	[11 064.60]		4
7	051	$(10)^{-}5$	[11 199.38]		11
8	080	$(00)^{+}8$	[11 213.30]		2
7	230	$(20)^{+}3$	11 734.525057	515	68
7	131	$(20)^{-}3$	11 774.707602	383	103
7	032	$(11)^{+}3$	11 963.537158	515	73
7	310	$(30)^{+}1$	12 106.977658	515	98
7	211	$(30)^{-}1$	12 116.797060	528	133
8	160	$(10)^{+}6$	[12 337.60]		1
7	112	$(21)^{+}1$	12 372.705608	420	103
9	090	$(00)^{+}9$	[12 488.02]		1
7	013	$(21)^{-}1$	12 520.122915	48	110
8	061	$(10)^{-}6$	[12 538.46]		2
8	*240*	*$(20)^{+}4$*	[*13 167.72*]		

Author's personal copy

Table 5 (*continued*)

P	$v_1v_2v_3$	$(mn)^{\pm}v_2$	VBO/cm^{-1}	Unc.	RL
8	141	$(20)^{-}4$	[13 212.70]		5
8	042	$(11)^{+}4$	[13 403.73]		1
8	221	$(30)^{-}2$	13 612.710202	49	74
9	*170*	$(10)^{+}7$	[*13 617.64*]		
8	320	$(30)^{+}2$	[13 602.66]		17
8	400	$(40)^{+}0$	[13 793.??]		61
8	301	$(40)^{-}0$	13795.398204	49	94
9	071	$(10)^{-}7$	[13 795.41]		1
8	122	$(21)^{+}2$	[13 870.46]		11
8	023	$(21)^{-}2$	[14 015.48]		13
8	202	$(31)^{+}0$	14 187.982458	1390	49
8	103	$(31)^{-}0$	14 276.336127	525	68
8	004	$(22)^{+}0$	[14 488.22]		3
10	*081*	$(10)^{-}8$	[*14 928.35*]		
10	*260*	$(20)^{+}6$	[*5 825.03*]		
10	*161*	$(20)^{-}6$	[*15 916.60*]		
10	340	$(30)^{+}4$	[16 487.09]		7
10	241	$(30)^{-}4$	[16 496.68]		2
10	142	$(21)^{+}4$	[16 742.51]		8
10	321	$(40)^{-}2$	16 775.380902	1459	28
10	420	$(40)^{+}2$	[16 776.79]		18
10	500	$(50)^{+}0$	[16 854.77]		28
10	401	$(50)^{-}0$	16 854.990902	1459	44
10	043	$(21)^{-}4$	[16 905.63]		2
10	222	$(31)^{+}2$	[17 173.30]		7
10	*123*	$(31)^{-}2$	[*17 258.83*]		
10	302	$(41)^{+}0$	[17 416.76]		1

[a] See footnotes a and b to Table 4.

here use was made of the known dependence of the rotational energies on rotational quantum numbers [123]. Of course, if more than one electronic state is considered, an extra label should be used to distinguish between these electronic states.

Finally, we note that while the quantum numbers assigned here are used largely as a book-keeping exercise, in other contexts their values can be important. This is particularly true for pressure broadening parameters, where semi-empirical models are often based on the use of these quantum numbers [124].

The structure of the energy levels of the $H_2{}^{17}O$ and $H_2{}^{18}O$ molecules is very similar to that of $H_2{}^{16}O$. Consequently, for $H_2{}^{17}O$ and $H_2{}^{18}O$, the quantum number labeling could be performed on the basis of the quantum numbers already determined for the energy levels of the $H_2{}^{16}O$ molecule. There were only a few occasions during our validation procedure where the quantum labels had to be changed. Nevertheless, the situation is much more complicated for the main isotopologue to be considered later due to the greater number and range of observed transitions for $H_2{}^{16}O$. From here on, the use of the approximate labels given in Tables 4 and 5 and the supplementary data is advised for all studies of the spectra of water vapor.

2.3. Origins of the Spectroscopic Networks

The energy levels of $H_2{}^{17}O$ and $H_2{}^{18}O$ are divided into a *para* and an *ortho* SN. By construction, the lowest level within each SN has a value of zero, so that the energy zero is defined unequivocally and with an associated uncertainty of zero. MARVEL results in the correct energy levels in an absolute sense for SNs not connected to the fundamental level only if the value of the lowest-energy level within the higher-energy SN, zero by definition of the SN, is shifted to the correct transition energy. Since, due to the appropriate selection rules, this transition cannot be measured directly (otherwise the two SNs would not be distinct), the difference, which might be called the spectroscopic network origin (SNO), must be estimated based on empirical and/or theoretical considerations. Due to the availability of approximate rotational Hamiltonians, which are highly accurate for the lowest levels, this presents no hindrance in the determination of highly accurate absolute energy levels for the *para* and *ortho* SNs of water.

Due to the nature of the spectroscopic measurements, the grand list of experimental transitions may contain so-called floating SNs (FSNs), which involve transitions that have no linkage with the origins of the theoretically distinct SNs. The correct absolute values of these FSN energy levels cannot be computed with MARVEL alone, just their relative values within the FSN. These FSNs can be divided into two parts: disjoint sets and orphans (ORP). If a given energy level has only one partner and this energy level and its partner belong to one and only one transition then these two energy levels are called orphans. Energy levels which are members of none of the principal SNs and are not orphans either are placed in one of the

Author's personal copy

many FSNs. The purpose of an underlying tree-building algorithm within MARVEL is to put each energy level into one of the transition families (SNs, FSNs, and ORPs).

2.4. W@DIS

The distributed information system W@DIS [13,14], one of the intended end products of the effort of this IUPAC TG, can be accessed via http://wadis.saga.iao.ru. W@DIS is aimed at (a) collecting all kinds of original information about the high-resolution spectroscopy of the water molecule, (b) providing active storage of these data and related metadata, and (c) delivering the collected and related information to users in several different forms, all via the Internet. The W@DIS system comprises three types of data structures (DS). The first one stores energy levels and related metadata for isolated molecules, in this case those of water. The second DS allows storage of information about transition wavenumbers. The third DS is used for storing line parameters, including line intensities, collisional half-widths, pressure shifts, and so on. Each DS allows storage of results related to the solution of the direct or the inverse problems of high-resolution molecular spectroscopy. The DS described form the basis for construction of data retrieval systems (for example, that related to HITRAN [3]). Each information source within W@DIS has a dataset, a semantic metadata set, and a commentary. Semantic metadata describe the details of the dataset as given in the source (spectral interval, values of physical characteristics, method of calculation, and so on). Commentaries comprise unstructured data represented by a natural language.

Since new experimental data on water vapor appear regularly in the literature, the energy levels and transition sets processed by MARVEL will be updated regularly and made available through W@DIS.

3. Sources of elementary transition data

In selecting papers to use in the MARVEL processes, only sources of primary transition data have been considered. That is, results from published spectroscopic measurements that include details of the experimental procedure. Secondary data, such as tabulated energy levels or Hamiltonian fits, were not considered except occasionally for checking purposes. Within this framework, we have attempted to be as comprehensive as possible, although we were forced to exclude some work where the actual transition data are not given. In a few cases, documented in Tables 2 and 3, early work has also been disregarded where the uncertainties were large compared to modern measurements. In general, however, we have included multiple, distinct measurements (as opposed to refits of the same measurements) of transitions as this aids the precision with which the levels can be determined.

We note that pure rotational transitions are usually measured with much lower relative and absolute uncertainties than vibration–rotation transitions. This means that obtaining a complete, reliable set of measured pure-rotation transitions is of great importance for establishing the reliability of the complete set of energy levels for a given isotopologue. Given the relatively small number of modern measurements of pure-rotational transitions, the oldest data sources used here usually involve measurements of such transitions.

3.1. Experimental techniques

There are a considerable number of spectroscopic techniques which have been used to measure rovibrational lines of water vapor. While it is not our purpose to review such techniques here, a few remarks related to the accuracy of lines and the resulting levels are appropriate.

Tables 2 and 3 provide for each data source the experimental method and the physical conditions related to the recording of the spectra. Due to the large number of related experimental studies, nearly continuous coverage has been achieved up to 17 125 cm^{-1} for both $H_2{}^{17}O$ and $H_2{}^{18}O$. As modern measurements of pure rotational transitions are very scarce, the pure-rotational transitions were mostly obtained from early works and are limited to a small number.

Most of the spectra were obtained by Fourier transform spectroscopy (FTS), which has allowed a wide spectral coverage from the microwave region to the near ultraviolet. In order to detect weak lines, FTS spectrometers have been equipped with long multipass cells. Absorption path lengths as long as 433 and 1804 m have been achieved with the cells available at Kitt Peak and Reims, respectively, providing a large number of observed transitions, mostly in the near infrared (NIR) region.

Laser-based methods, such as CRDS (cavity ringdown spectroscopy) and ICLAS (intracavity laser absorption spectroscopy), are limited to certain spectral regions depending on the availability of tunable laser sources. These techniques have specific advantages in terms of sensitivity and spectral resolution, which make them particularly suitable for the characterization of spectral regions with weak absorption features. This is why extensive investigations with laser-based methods were mostly limited to transparent atmospheric windows or to the visible region. A further advantage of these methods in the case of the minor isotopologues of water considered is that they require a small quantity of gas and then allow a very high isotopic enrichment which is of great help for the spectral analysis.

In spite of the small natural abundances of the two isotopologues considered ($H_2{}^{17}O$: 0.000372 and $H_2{}^{18}O$: 0.00199983), part of the data were obtained from spectra recorded with water in natural abundance (see Tables 2 and 3). It is also worth

Author's personal copy

mentioning that while the large majority of spectra are absorption spectra recorded at room temperature, some emission spectra of $H_2{}^{18}O$ heated over 1000 K are available [41,104].

3.2. Uncertainties of lines and levels

Measurement uncertainty is a combination of precision and absolute accuracy. Precisions of measured positions vary according to the type and quality of the spectrometer, the spectral resolution relative to the observed line width, the signal to noise ratio, the choice and control of experimental conditions, the complexity of the spectrum, and the retrieval methods. Precisions are first evaluated by reproducibility (obtaining a similar value from several different spectra) and later by comparison with correctly calculated theoretical or MARVEL-type values.

Precisions of line positions will represent the absolute accuracies of the measurements, provided the calibration standards themselves are reliable and have much better precision than the targeted species. However, inconsistencies and errors in the standards introduce offsets in the absolute accuracies which degrade the overall precision. Measurement errors usually remain undiscovered until experiments are repeated by others. Once recognized, such errors can sometimes be corrected; this was the case when the quality of infrared calibration standards was reviewed by Guelachvili et al. [113].

Some precisions remain degraded by effects beyond the control of the present IUPAC endeavor. These include experiments done with high gas pressures that cause pressure-induced shifts in the line centers that can be both negative and positive. In fact, some of the short wavelength data were taken with different foreign gases in the sample. In addition, in older studies positions were retrieved with automated line-center algorithms (using first and second derivatives) which poorly represent blended features. The now commonly used interactive curve-fitting algorithms produce better precisions for positions (and intensities).

In the present effort, renormalization of some calibrations, in order to preserve the inherent precisions of the reported line positions, was considered. Due mostly to the limited availability of overlapping measurements for the minor isotopologues of water considered, this undertaking needed no recalibration. The only case where recalibration was employed concerned the line position data of 83Guelachv [42], where the calibration factor introduced in Ref. [113] was confirmed by MARVEL and thus was used unchanged.

Apart from optimism (or occasional pessimism) on the part of executors of experiments when assigning uncertainties to the measured lines, the uncertainties within the set of measured transitions assembled from different sources might suffer from sizeable systematic errors.

After cleansing of the database and applying the iterative robust weighting algorithm of MARVEL, a database was created containing self-consistent and correctly assigned transitions and the seemingly best possible related uncertainties. Energy levels, and their uncertainties, determined from these transitions are in harmony with the measured transitions and their (adjusted) uncertainties.

3.3. Comments on the data sources for $H_2{}^{17}O$

(2a) 71StBe: Hyperfine components of two rotational transitions are given.

(2b) 75DeHe: This reference also contains the two transitions measured in Ref. [26]. Actually there are 14 hyperfine components measured in Ref. [26].

(2c) 99MaNaNaOd: Very high accuracy results obtained with a far infrared spectrometer using a tunable radiation source. Independently from this study, these transitions have been validated and analyzed in Ref. [12]. While the analysis was carried out in MHz in Ref. [12], the results were reported in cm^{-1} using a conversion factor of 29 979.25 instead of the fully correct factor of 29 979.2458 employed here. This fact explains some of the slight differences between the results of this study and those of Ref. [12].

(2d) 81Partridg: The experimental apparatus was a phase modulated NPL-Grubb Parsons Cube interferometer. The abundances of the $H_2{}^{16}O$, $H_2{}^{17}O$, and $H_2{}^{18}O$ isotopologues in the sample were 74%, 10%, and 16%, respectively.

(2e) 78KaKaKy: Michelson-type double-beam FTS with a path difference of 50 cm. Pressures were between 0.4 and 4 Torr of natural abundance water vapor. Two measured transitions, at 301.302 and 301.305 cm^{-1}, proved to be incompatible with the variational results employed in this study and thus were not considered for further analysis.

(2f) 80KaKy: The abundances of the $H_2{}^{16}O$, $H_2{}^{17}O$, and $H_2{}^{18}O$ isotopologues in the sample were 47%, 24%, and 29%, respectively. Rotational assignment of the lower energy level of the transition 80KaKy.234 had to be changed from [8 4 4] to [8 4 5]. Two measured transitions, at 396.8046 and 465.2015 cm^{-1}, proved to be incompatible with the variational results employed in this study and thus were not considered for further analysis.

(2g) 77Winther: Modified Beckman/RIIC FS.720 Michelson interferometer with resolution in the range of $0.08-0.15\,cm^{-1}$ was used. Pressures were between 0.5 and 17.8 Torr of natural abundance water vapor. Five measured transitions, at 61.437, 75.184, 165.988, 276.366, and 301.581 cm^{-1}, proved to be incompatible with the variational results employed in this study and thus were not considered for further analysis.

(2h) 83Guelachv: Due to a calibration problem, the original reported transitions have been scaled in this study by a scale factor of 0.999 999 770 [113]. In the MARVEL input file only the scaled transitions, with the original uncertainties, have been included.

Author's personal copy

(2i) 71WiNaJo: A 3.5-m Littrow-type vacuum infrared spectrograph was used for recording the spectra. The spectral resolution was not better than 0.04 cm^{-1}. No information on pressure, temperature, path length and isotopic abundances is given. Twenty-two measured transitions proved to be incompatible with the variational results employed in this study and thus were not considered for further analysis.

(2j) 78JoMc: Saturated absorption by CO laser Stark spectroscopy. One measured transition, at 1643.5715 cm^{-1}, proved to be incompatible with the variational result employed in this study and thus was not considered for further analysis. Rotational assignment of the lower energy level of the other transition had to be changed from [1 0 0] to [1 0 1].

(2k) 94Totha: The spectra were obtained with FTS located at the Kitt Peak National Observatory. Percent abundance of isotopic species: $H_2{}^{16}O$—4.0–99.6%, $H_2{}^{17}O$—0.04–57.7%, $H_2{}^{18}O$—0.2–94.0%.

(2l) 69FrNaJo: $H_2{}^{17}O$ transitions observed in an $H_2{}^{18}O$-enriched sample. One transition, at 3846.707 cm^{-1}, had to be deleted from the list of input transitions since this is a forbidden *ortho–para* transition. Eight measured transitions, at 3529.229, 3581.377, 3694.266, 3727.513, 3742.086, 3747.606, 3832.764, and 3942.407 cm^{-1}, proved to be incompatible with the variational results employed in this study and thus were not considered for further analysis.

(2m) 73CaFlGuAm: Two measured transitions, at 3581.5497 and 3581.89324 cm^{-1}, proved to be incompatible with the variational results employed in this study and thus were not considered for further analysis.

(2n) 83PiCoCaFl: High-temperature absorption spectrum recorded with a tunable difference frequency laser spectrometer.

(2o) 07JeDaReTy: Two measured transitions, at 4348.9402 and 5160.3520 cm^{-1}, proved to be incompatible with the variational results employed in this study and thus were not considered for further analysis.

(2p) 77ToFlCaa: $H_2{}^{17}O$ transitions observed in an $H_2{}^{18}O$-enriched spectrum. Thirteen measured transitions, at 5178.941, 5195.341, 5197.934, 5206.827, 5207.520, 5215.617, 5266.372, 5317.453, 5342.893, 5417.143 (twice), 5423.766, and 5498.595 cm^{-1}, proved to be incompatible with the variational results employed in this study and thus were not considered for further analysis.

(2q) 04MaRoMiNa: Two measured transitions, at 6694.4898 and 6698.0387 cm^{-1}, proved to be incompatible with the variational results employed in this study and thus were not considered for further analysis.

(2r) 94Tothb: Five measured transitions, at 7259.764, 7278.127, 7344.903, 7414.205, and 7432.8943 cm^{-1}, proved to be incompatible with the variational results employed in this study and thus were not considered for further analysis. Approximate assignments of two transitions, at 7441.817 and 7276.907, were corrected based on 05ToTe and the variational results.

(2s) 77ToFlCab: Six measured transitions, at 7107.438, 7220.087, 7222.305, 7282.003, 7328.607, and 7333.257 cm^{-1}, proved to be incompatible with the variational results employed in this study and thus were not considered for further analysis.

(2t) 05ToTe: Experimental spectra reported by Schermaul et al. [115] were analyzed here. Five measured transitions, at 7462.729, 8253.517, 8460.419, 8512.331, and 8643.986 cm^{-1}, proved to be incompatible with the variational results employed in this study and thus were not considered for further analysis.

(2u) 06LiHuCaMa: The abundances of the $H_2{}^{16}O$, $H_2{}^{17}O$, and $H_2{}^{18}O$ isotopologues in the sample were 79%, 5%, and 16%, respectively. In many cases the artificially low reported uncertainties have been increased to 0.001 cm^{-1}.

(2v) 99CaFlMaBy: Analysis of FTS spectra reported in Refs. [85,87]. Five transitions, at 10 256.2215, 10 661.0808, 10 713.8278, 10 746.9244, and 10 903.7925 cm^{-1}, proved to be incompatible with the variational results employed in this study and thus were not considered for further analysis.

(2w) 05TaNaBrTe: Analysis of FTS spectra recorded at Kitt Peak. The reported data contains a forbidden transition at 12 272.384 cm^{-1}. Eleven transitions, at 11 929.9138, 11 971.0539, 11 984.8573, 12 362.708, 12 481.593, 12 483.2502, 13 666.513, 13 730.9582, 13 931.492, 13 934.3082, and 14 395.9773 cm^{-1}, proved to be incompatible with the variational results employed in this study and thus were not considered for further analysis.

(2x) 07MaToCa: $H_2{}^{17}O$ transitions observed in an $H_2{}^{18}O$-enriched spectrum. One transition, 07MaToCa.213 at 12 425.3461 cm^{-1}, was manually deleted from the list of transitions. 07MaToCa.118 shows the correct value of this transition, consequently, this appears to be a misprint in the original dataset. Thirteen transitions, at 11 919.3473, 11 927.1617, 11 970.1617, 11 977.1403, 12 251.7326, 12 300.170, 12 331.3884, 12 366.8994, 12 425.3461, 12 428.9413, 12 434.8038, 12 487.4677, and 12 563.1453 cm^{-1}, proved to be incompatible with the variational results employed in this study and thus were not considered for further analysis.

(2y) 06NaSnTaSh: This dataset contains one forbidden transition at 17 036.48 cm^{-1}. The 38 transitions rejected based on the combination differences and/or comparison with the variational results employed in this study and thus were not considered for further analysis are reported in the Supplementary Material.

3.4. Comments on the data sources for $H_2{}^{18}O$

(3a) 06GoMaGuKn: Ten hyperfine components of six rotational *ortho* and *para* transitions measured between 203 407.498 and 547 676.470 MHz.

(3b) 87BeKoPoTr: The first observation of the rotational transitions in the (0 1 0) vibrational state. A microwave spectrometer of the Institute of Applied Physics (Russia) was used. Water vapor samples 20% enriched by $H_2{}^{18}O$ at pressures between 0.3 and 0.6 Torr were used.

Author's personal copy

(3c) 76FlGi: One transition, at 33.4915 cm^{-1}, was rejected using combination difference relations.

(3d) 99MaNaNaOd: A NPL-Grubb Parsons Cube interferometer was used. Spectra have been recorded at a resolution of 0.07 cm^{-1}. Pressures: 18 Torr (natural water vapor), 14 Torr (1:1 mixture H_2O/D_2O), and 10 Torr (95% enriched D_2O). After deuterated experiments the spectra of 90% enriched $H_2{}^{18}O$ at 16 Torr were recorded. The original measurements are between 554 859.748 and 5 240 714.945 MHz. A special MARVEL reanalysis of these transitions, resulting in modified uncertainties, has been given in Ref. [12]. While the analysis was carried out in MHz in Ref. [12], the results were reported in cm^{-1} using a conversion factor of 29 979.25 instead of the fully correct factor of 29 979.2458 employed here. This fact explains some of the slight differences between the results of this study and those of Ref. [12].

(3e) 80KaKy: See comment (2f) to Table 2. One transition, at 303.1096 cm^{-1}, was rejected based on combination difference relations.

(3f) 77Winther: See comment (2g) to Table 2. Rejection of the transitions was based on combination difference relations.

(3g) 78KaKaKy: See comment (2e) to Table 2. One transition, at 335.1577 cm^{-1}, was rejected based on combination difference relations.

(3h) 69BePoTo: Ten lines in the 178−398 cm^{-1} region have been observed in a 3-m-long pulsed $H_2{}^{18}O$ discharge. Operating pressures and voltages are typical to those for water-vapor lasers. Five transitions, at 205.74, 206.76, 282.62, 376.01, and 397.42 cm^{-1}, were rejected based on combination difference relations.

(3i) 03MiTyMe: The FIR emission spectrum of heated water vapor up to 1370 K has been recorded at a resolution of 0.0055 cm^{-1} using a Bruker IFS 120 HR FTS. Measurement was done in a fused quartz cell with an effective length of hot gas of about 60 cm. A number of degenerate high J and high K_a transitions, with appropriate labels, have been added for which only one label was provided in the original article. Therefore V is larger than A because the originally reported list of transitions was extended with degenerate transitions.

(3j) 92Toth: One transition, at 1244.78805 cm^{-1}, was rejected based on combination difference relations.

(3k) 83Guelachv: See comment (2h) to Table 2.

(3m) 71WiNaJo: See comment (2i) to Table 2. Rejection of the transitions was based on combination difference relations.

(3n) 78JoMc: Hyperfine components of two transitions measured at 1640.176 and 1693.7326 cm^{-1}.

(3o) 75ToMa: The spectrum was recorded with a 1.8 m Jarrel-Ash grating spectrometer. The sample mixture ratio of $H_2{}^{18}O$ to $H_2{}^{16}O$ was 1:1 and the $H_2{}^{17}O$ impurity was 0.1% of the sample. The path lengths ranged from 8 to 40 m and the sample pressures ranged from 2 to 8 mmHg with the gas samples at room temperature. The spectral resolution was about 0.07 cm^{-1} for the region 2900 to 3240 cm^{-1} and about 0.04 cm^{-1} for the region 3240 to 3400 cm^{-1}. Rejection of the transitions was based on combination difference relations.

(3p) 94Totha: See comment (2k) to Table 2.

(3q) 69FrNaJo: Assignment of the transition 3946.796 (69FrNaJo.40) is incorrect as the stated $8_{54} \rightarrow 7_{53}$ transition is not allowed. The 10_{63} label of the lower-level assignment of the transition at 3451.800 (69FrNaJo.555) is incorrect. Consequently, both transitions have been deleted by the test facility of MARVEL. Rejection of all the other transitions was based on combination difference relations.

(3r) 83PiCoCaFl: See comment (2n) to Table 2. Rejected transitions at 3801.576 and 3839.859 cm^{-1}, based on combination difference relations.

(3s) 73CaFlGuAm: Three transitions, at 3713.96818, 3747.49352, and 3857.82791 cm^{-1}, were rejected based on combination difference relations.

(3t) 83ToBr: Fourier transform spectra of HDO recorded in a 25-cm long absorption cell with spectral resolution of 0.01 cm^{-1} at room temperature. Two different gas mixtures, Set1 (50% HDO, 25% H_2O, 25% D_2O) and Set2 (28% HDO, 69% H_2O, 3% D_2O) were used. The total sample pressures of Set2 were 16.15, 7.79, and 4.35 Torr, and those for Set1 were 12.05, 7.9, and 1.2 Torr. Only three $H_2{}^{18}O$ lines (3717.8121, 3730.6801, and 3738.02392 cm^{-1}) were observed in these spectra.

(3u) 07JeDaReTy: Five transitions, two at 4283.9684, and one at 5322.5782, 5963.7585, and 6301.9509 cm^{-1}, have been rejected based on combination difference relations. In many cases the artificially low reported uncertainties have been increased to 0.001 cm^{-1}.

(3v) 85ChMaFlCa: The FTS at the Kitt Peak National Observatory was used for recording spectra of ^{18}O-enriched water. The (total pressures/atm and absorption paths/cm) for the different recordings were (0.00101 and 2494), (0.00368 and 4900), and (0.00368 and 21 742).

(3w) 86ChMaFlCa: Two Fourier transform spectra recorded in Ref. [83] were used for assignment of the hot band $2\nu_2+\nu_3-\nu_2$ of ^{18}O-enriched water. The (total pressures/atm and absorption paths/cm) for different records were (0.00101 and 2494), (0.00368 and 4900), and (0.00368 and 21 742). Assignments from this paper were prefered to those of Ref. [91].

(3x) 77ToFlCaa: The spectrum was recorded with a 1.8 Jarrel-Ash grating spectrometer. The starting sample mixture ratio of $H_2{}^{18}O$ to $H_2{}^{16}O$ was 1:1 and the $H_2{}^{17}O$ impurity was 0.1% of the sample. The path lengths ranged from 8 to 48 m and the sample pressure and temperature were 2.3 Torr and 296 K, respectively. Rejection of the transitions was based on combination difference relations.

(3y) 06LiDuSoWa: Absorption spectra of ^{18}O-enriched water have been recorded using a Bruker IFS 120 HR spectrometer. The pressure was between 11 and 1307 Pa. Rejection of the transitions was based on combination difference relations. The transition at 4012.96 cm^{-1} was deleted as the same assignment is repeated for a line at 4012.93 cm^{-1} which shows a better obs − calc tendency.

Author's personal copy

(3z) 86ChMaCaFlb: The FTS at the Kitt Peak National Observatory was used for recording six spectra of ^{18}O-enriched water. The total pressure values were between 0.00101 and 0.00618 atm and absorption path from 2494 to 21 742 cm. One spectrum of natural abundance of $H_2{}^{18}O$ with pressure of 0.00197 atm and path length of 43 396 cm was also recorded. Rejection of the transitions was based on combination difference relations.

(3aa) 06LiNaSoVo: The absorption spectra of ^{18}O-enriched water have been recorded using a Bruker IFS 120 HR spectrometer. The spectra were recorded at different pressure and path lengths: 11 Pa × 15 m, 215 Pa × 15 m, 1307 Pa × 15 m, and 1307 Pa × 105 m. Rejection of the transitions was based on combination difference relations. The transition at 6797.06 cm^{-1} showed a bad obs – calc tendency.

(3bb) 04MaRoMiNa: The absorption spectra of natural abundance water vapor between 1.48 and 1.63 μm at room temperature have been recorded using CW-cavity ring down spectroscopy. Pressure value was 17 Torr in the whole spectral region. Additional recordings at 1 Torr of pressure were performed above 6510 cm^{-1} due to the presence of too strong lines. Rejection of the transitions was based on combination difference relations and comparison with variational computations.

(3cc) 94Tothb: Three transitions, at 7036.823, 7046.413, and 7347.872 cm^{-1}, were rejected based on combination difference relations.

(3dd) 77ToFlCab: See comment (3s) to this table. Two transitions, at 7037.313 and 7184.455 cm^{-1}, were rejected based on combination difference relations.

(3ee) 05ToTe: See comment (2t) to Table 2. Rejection of the transitions was based on combination difference relations and, in the case of 7430.744301 cm^{-1}, by comparison with the results of the variational computations.

(3ff) 06LiHuCaMa: FTS spectra enriched in ^{18}O and ^{17}O were recorded in the 8012–9336 cm^{-1} region in Hefei (China) and in the National Solar Observatory (Kitt Peak, AZ, USA), at near room temperature. The sample of water vapor enriched to 95% ^{18}O was used for recording the spectra below 12 000 cm^{-1} in Hefei. Several spectra have been recorded with pressures of 215 and 1307 Torr and with absorption path lengths of 15 and 105 m at 0.015 cm^{-1} resolution. The ^{18}O-enriched (73% ^{18}O and 27% ^{16}O), the ^{17}O-enriched (5% ^{17}O, 16% ^{18}O, and 79% ^{16}O) and the natural abundance water vapor spectra in the 8500–9330 cm^{-1} region were recorded at Kitt Peak. Rejection of the transitions was based on combination difference relations and, in the case of 8857.5729 cm^{-1}, by comparison with the results of the variational computations.

(3gg) 87ChMaFlCa: The FTS at the Kitt Peak National Observatory was used for recording four spectra of ^{18}O and ^{17}O enriched water. One spectrum of natural abundance of $H_2{}^{18}O$ with pressure of 0.00197 atm and path length of 14 524 cm with resolution 0.01 cm^{-1} was also recorded. Rejection of the transitions was based on combination difference relations. The transition at 10 546.17 cm^{-1} showed a bad obs – calc tendency.

(3hh) 07MaToCa: The conditions of the ICLAS experiments correspond to an equivalent absorption path length of 4.8 and 14.4 km. The $H_2{}^{16}O$to $H_2{}^{18}O$ ratio in the sample was about 45–55%. Rejection of the transitions was based on combination difference relations. A number of degenerate high J and high K_a transitions, with appropriate labels, have been added for which only one label was provided in the original article.

(3ii) 95ByNaPeSc: The FTS at the Kitt Peak National Observatory was used for recording of ^{18}O-enriched water vapor spectra in the 11 300−13 600 cm^{-1} spectral region. One spectrum of natural abundance of water species was also recorded in order to assign the lines of $H_2{}^{16}O$. Rejection of the transitions was based on combination difference relations and, in the case of 12 213.6854 cm^{-1}, by comparison with results from variational computations.

(3jj) 05TaNaBrTe: Analysis of the spectra reported in Refs. [83,84,87,115] and numerous mistakes of a previous study [103] have been corrected. The transition at 13 681.2733 cm^{-1} had to be deleted as no assignment is given. Rejection of other transitions was based on combination difference relations and by comparison with results from variational computations.

(3kk) 04TaSnUbTe: Cavity ring-down spectrometer with a cell 86.5 cm long was used for recording absorption spectra of $H_2{}^{18}O$. Rejection of the transitions was based on their comparison with results from variational computations.

4. MARVEL energy levels

4.1. $H_2{}^{17}O$

The $H_2{}^{17}O$ energy levels and uncertainties presented here are not identical to those published in Ref. [10], the previous best compilation of such data. The number of transitions considered increased by more than 1000, due to the inclusion of new data sources, such as 07MiLeKaCa [68] and 07JeDaReTy [67], and also by the inclusion of older references which were not considered in Ref. [10]. Even more substantially, the experimental information contained in the SISAM database [40] was replaced by the line information provided in the original publications of Toth and co-workers: 77ToFlCaa [29], 77ToFlCab [30], 92Toth [44], 93Totha [45], 94Totha [46], 94Tothb [47], 98Toth [49], 05Totha [58] and 05Tothb [59]. The extensions in the input file meant that the previously detected FSNs disappeared, and all measured transitions now belong either to the *ortho* or *para* SN. Furthermore, all orphans disappeared as they could be connected to the principal SNs.

As is clear from Table 4, the limited number of experimental data available means that pure bending transitions with a bending quantum number larger than 2 have not been determined. The largest J value for which term values have been

Author's personal copy

determined experimentally is 17. While this is a relatively high value, the coverage of higher-J rotational levels is scarce at best for this isotopologue.

In the case of $H_2{}^{17}O$, the lowest energy level of the *ortho* SN is the 1_{01} rotational state. The corresponding SNO, i.e., the difference between the 0_{00} state of the *para* SN and the 1_{01} state of the *ortho* SN, 23.773510 cm^{-1}, was obtained from 94Totha [44].

The maximum polyad number, P, for which VBOs have been determined is 10. The complete list of VBOs, on the other hand, is available only for $P = 0-2$. For $P \geqslant 3$, first the pure bending VBOs are missing ($P = 3$ and 4), then mixed levels with highly excited bends (e.g., (1 3 0) and (0 3 1) for $P = 5$). For $P \geqslant 4$, with the exceptions of (1 3 1) and (0 7 1), no VBOs with a bending excitation larger than 2 have been assigned. Clearly, it is much easier to assign the more or less pure stretching states even at lower energies. For $P = 6$ only one vibrational state, (1 4 0), has no associated rotational data, while already for $P = 9$ 14 VBOs are not determined out of the total of 15. Interestingly, 14 out of the 21 $P = 10$ levels support at least one rovibrational level.

Based on the symmetry information available from variational computations and the polyad structure, checking the labeling of the VBOs provided by MARVEL proved to be straightforward. The only surprise in the vibrational labeling concerns the (4 2 0)–(3 2 1) pair. Since these states have different symmetries, one must accept the variational result that, unlike in all other cases studied, the (3 2 1) state has a lower energy than the (4 2 0) state. Note that this holds for the isotopologues $H_2{}^{16}O$, $H_2{}^{17}O$, and $H_2{}^{18}O$.

There are only very few measured transitions whose labelling was so inaccurate that they had to be deleted prior to even running MARVEL. It is not clear what the source of the observed discrepancies is. As detailed below, rather more transitions were deleted once the results of the MARVEL run were available.

There is a surprisingly large number of transitions, 595 out of the total of 8614, whose originally stated uncertainties increased by more than 10-fold during the reweighting protocol. The only sources where there were no such cases are 71StBe [21], 99CaFlMaBy [51], 02MiTyStAl [53], and 83PiCoCaFl [41]. The worst offenders in this sense are 80KaKy [35] (with 123 such uncertainties out of a total of 373), 06NaSnTaSh [65] (with 102 such uncertainties out of a total of 513), and 07MiLeKaCa [68] (with 60 such uncertainties out of a total of 235).

4.2. $H_2{}^{18}O$

For $H_2{}^{18}O$ the number of validated SN1 and SN2 energy levels are 2199 and 2650, respectively. The largest J value for which term values have been determined experimentally is 20. VBOs with bending excitation larger than four have not been determined.

As apparent when comparing Tables 4 and 5, considerably more VBOs have been determined experimentally for $H_2{}^{18}O$ than for $H_2{}^{17}O$. When the difference between the two sets of VBOs are available, they clearly show the expected decrease, due to the larger mass of ^{18}O as compared to ^{17}O, and the two sets basically confirm each other.

In the case of $H_2{}^{18}O$, similarly to $H_2{}^{17}O$, the lowest energy level of the *ortho* SN is the 1_{01} rotational state. The corresponding SNO is 23.754902 cm^{-1} and was taken from 92Toth [44].

The maximum polyad number, P, for which VBOs have been determined is 10. The complete list of VBOs, on the other hand, is available only for $P = 0-3$. For $P \geqslant 4$, first the pure bending VBOs are missing ($P = 4$ and 5), then mixed levels with highly excited bends (e.g., (1 4 0) for $P = 6$).

4.3. Accidental degeneracies

For symmetric isotopologues of water, high-J energy levels have many (near) degeneracies between states with *ortho* and *para* symmetry [18]. For $H_2{}^{16}O$ these accidental degeneracies are well established [9]; indeed, there has even been discussion on why water does not form fourfold degeneracies for higher rotational states [125]. There are two possible uses of these degeneracies within the context of the present study.

First, in principle one could use these observations to fix the *ortho* to *para* SNO. However, it seems more justified to use this possibility as a control test on whether the original choice of the SNO was correct and not to use it in a direct way to merge distinct SNs. Second, the presence of energy levels predicted to be almost degenerate on the basis of variational calculations can provide a method of characterising further energy levels. Indeed, this property was found important for attaching FSNs in the previous similar study on $H_2{}^{16}O$ [9].

Table 6 provides an extensive list of those levels of $H_2{}^{17}O$ for which the MARVEL procedure resulted in near degeneracies and these degeneracies have been confirmed by extensive nuclear motion computations. Furthermore, a table in the Supplementary Material provides a full list of those levels of $H_2{}^{17}O$ which are predicted to be quasi-degenerate in the variational nuclear motion calculations but for which only one component of the pair has been determined by MARVEL. Note that for the purpose of these tables quasi-degeneracy was defined as a splitting of less than half the uncertainty with which MARVEL determines the single level.

As can be checked in the Supplementary Material, the degeneracies found for the VBOs hold very well both in the MARVEL and in the variational results. Another feature is that the MARVEL and the variational differences often have

Author's personal copy

Table 6
$H_2{}^{17}O$ energy levels, in cm^{-1}, arranged by increasing J and predicted to be quasi-degenerate by variational nuclear motion calculations (VAR) for which the MARVEL procedure, based on the available experimental measurements, yields only one level.

$v_1 v_2 v_3$	State 1			State 2		$E_1^{VAR} - E_2^{VAR}$
	$J\ K_a\ K_c$	E_1^{MARVEL}	E_1^{VAR}	$J\ K_a\ K_c$	E_2^{VAR}	
030	441	5328.161219	5328.195453	440	5328.203949	−0.008497
040	441	6902.216295	6902.219992	440	6902.224488	−0.004496
012	550	9723.926347	9723.943665	551	9723.939263	0.004403
003	551	11 669.654650	11 669.633753	550	11 669.642459	−0.008706
120	551	7634.150142	7634.163271	550	7634.166119	−0.002848
120	661	7980.735806	7980.764139	660	7980.764261	−0.000123
201	762	11 717.659472	11 717.661989	761	11 717.665969	−0.003980
301	762	14 885.761780	14 885.737371	761	14 885.746520	−0.009150
100	770	5007.494899	5007.579106	771	5007.579071	0.000034
101	771	8540.780006	8540.781219	770	8540.780332	0.000887
321	808	17 480.218709	17 480.198044	818	17 480.203419	−0.005374
021	853	8214.501181	8214.529125	854	8214.537723	−0.008598
101	871	8729.552283	8729.590701	872	8729.598848	−0.008147
100	872	5200.602380	5200.683551	871	5200.684027	−0.000476
200	881	8892.151110	8892.236793	880	8892.236807	−0.000014
013	919	13 412.976539	13 413.023715	909	13 413.014125	0.009590
001	982	5676.535523	5676.518639	981	5676.518810	−0.000170
013	10 010	13 596.386298	13 596.442784	10 110	13 596.445407	−0.002624
201	10 010	11 651.479882	11 651.489297	10 110	11 651.486573	0.002724
300	10 110	11 637.791712	11 637.821504	10 010	11 637.811702	0.009802
010	1092	4223.110623	4223.142319	1091	4223.142326	−0.000007
003	11 111	12 273.682661	12 273.734529	11 011	12 273.735368	−0.000839
201	13 112	12 527.091539	12 527.141639	13 212	12 527.133024	0.008615
101	13 113	8978.484723	8978.506739	13 013	8978.506632	0.000108
010	17 017	4544.655860	4544.594051	17 117	4544.594443	−0.000391

opposite signs. These sign differences appear random and show the limitations of variational nuclear motion computations based on empirically adjusted potential energy hypersurfaces.

The MARVEL energy levels reveal a few almost perfect degeneracies. A case where the difference between the *ortho* and *para* energy levels is less than $5 \times 10^{-6}\,cm^{-1}$ is (0 1 0) 6_{60} and 6_{61} at 2714.444174 for $H_2{}^{18}O$. No such degeneracies have been found for $H_2{}^{17}O$.

5. Variational validation of MARVEL energy levels

MARVEL gives the most dependable results when a particular energy level is at the center of a network of many transitions. Inevitably, there are always energy levels which are linked to the main network by a single transition, indeed in the case of branches there may be a series of such transitions. For these levels MARVEL can neither confirm the reliability of the experimental assignment nor give any reasonable uncertainty value if there are problems (for example, misrepresentation, misassignment, or mislabeling) with the experiment. The availability of MARVEL and variational energy levels for $H_2{}^{17}O$ and $H_2{}^{18}O$ allows the comparison of the assignments of the levels determined for these isotopologues as the differences between the MARVEL and variational energy levels are always smaller than the differences between neighboring energy levels of the correct symmetry. This comparison was made in order to remove those transitions from the MARVEL input which led to energy levels not supported by variational computations. Some of the transitions removed may correspond to correct experimental assignments but incorrect labels. Nevertheless, it was decided not to keep these transitions in order to arrive at a fully validated, dependable, and self-consistent set of levels and lines. After careful relabeling, the active feature of MARVEL can always be used to utilize these or any new transitions in a reanalysis of the data.

6. A comparison with HITRAN

For a discussion of comparisons of the results of this work (lines and levels) with data deposited in HITRAN, it is worth recalling the structure and quantities in the 2004 edition of the HITRAN database [3]. Table 2 of Ref. [3] presents the parameters (fields) that are contained in each transition (record) of the HITRAN linelist. The structure is in a text-file format of fixed-length records. The parameters contained in each transition are those that have been deemed necessary for input for calculating high-resolution absorption or radiance spectra through a gaseous media.

Author's personal copy

Table 7
Comparison of transition data found in the 2004 edition of HITRAN [3] and those used in the present compilation.

	$H_2{}^{17}O$	$H_2{}^{18}O$
Total number of validated transitions in present database	8614	29 364
Unique transitions in present database	6772	17 034
Number of validated SN1 transitions	3423	12 451
Number of validated SN2 transitions	5191	16 894
Transitions in HITRAN database	6120	9524
Concordant transitions[a]	4897	8515
Transitions differing by $>0.001\,cm^{-1}$	920	2252
Transitions differing by $>0.1\,cm^{-1}$	267	753
Transitions absent in present database	1223	1009
Transitions absent in HITRAN	1875	8519

[a] Unique transitions which are present both in HITRAN and in the present validated IUPAC database.

Table 7 compares the present results with data presented in HITRAN 2004. There are several notable differences between the HITRAN and the IUPAC water-vapor data analysis. First, HITRAN contains a mixture of observed and calculated entries, whereas the lines used in the present analysis are based strictly on published experimental values. Even though the goal in HITRAN is to have a complete set of self-consistent and maintainable values, in practice this is not possible at this time. Entries that have been determined under controlled laboratory conditions and are very accurate are frequently used in HITRAN. However, in order to have adequate sets of lines for important vibration–rotation bands, it is necessary to use theoretical extrapolations of the data (especially to the higher rotational levels), to have calculations of lines that are blended or obscured in laboratory observations, or to have calculations for quantities that theory actually yields better constrained values at present than experiment (some line-shape parameters, for example). Second, in the case of multiple sets of data for a quantity, HITRAN comes up with a single value. This consolidation of data has been made by judgment of the quality of the different datasets and means that all transitions in HITRAN are unique, i.e. are represented by a single entry. With the superior structure of the IUPAC database, all high-quality data have been retained. In principle a user can be given filtering codes to produce a smaller list for a specific application. Third, HITRAN is aimed at atmospheric temperature applications and, by application of a minimum transition intensity at 296 K, rejects many hot transitions; our present analysis aims to capture all transitions. The increased number of transitions in the present compilation is partly a reflection of this. To highlight these issues, a few differences between the HITRAN 2004 and the present IUPAC list of $H_2{}^{17}O$ transitions are mentioned below and are given in Table 7.

The extra transitions in HITRAN 2004 between 38 and 500 cm^{-1} came from calculations by Jucks [126]. The extra lines from 500 to 2261 cm^{-1} originated from calculations by Toth using the experimental energy levels of his own paper [49] and intensities also derived there. HITRAN 2004 cites Toth's website [40] for that material, and the values listed there are calculated not measured. The story with the lines in the $2261-8000\,cm^{-1}$ region is very similar. The transitions were calculated by Toth using data from his experiments in this spectral region over the years. While data above 8000 cm^{-1} came from spectra recorded using water in natural abundance, most came from the deciphering of old Kitt Peak spectra (long-path atmospheric absorption with the FTS) but these data have not been published.

7. Summary and conclusions

Among many other applications of such data, an extreme amount of high-quality molecular data are needed for the understanding of spectroscopic measurements related to different stars and the atmospheres of planets and exoplanets. One must know precise positions and often intensities and line shapes in order to be able to judge what is observed and how much of that species is present. Among the species for which spectroscopic data are needed for this or any other important scientific or engineering applications, water is probably the single most important molecule. Thus, the study of its complete spectrum is of prime importance. At the same time, this task provides a fertile testing ground for different experimental and theoretical approaches yielding the required information.

It would be convenient if high-resolution molecular spectroscopy experiments could yield the required line-by-line information. However, while experiments yield accurate and often precise data, the amount of information that can be obtained is only a small fraction of that required. Quantum theory, on the other hand, can result in the full information [11] but the accuracy of even the most sophisticated treatments [111] is considerably worse, especially for line positions, than that of experiments. Therefore, the best possible approach one can take is to use all the available experimental and quantum mechanical information to come up with a linelist as accurate as allowed by the available data.

While the ambitious task of this IUPAC TG has been to come up with a complete linelist for all isotopologues of water, the first step is to determine energy levels and line positions. This paper provides, for the first time, a dependable and carefully validated set of energy levels and transition wavenumbers, all with reliable and self-consistent uncertainties, for the minor water isotopologues $H_2{}^{17}O$ and $H_2{}^{18}O$. A brief summary of our results is provided in Table 8. As proven in this work, the MARVEL approach [10–12], combined with results from variational nuclear motion computations, provides an

Author's personal copy

Table 8
Summary of the validated MARVEL energy levels determined for the water isotopologues during the present study.[a]

SN	$H_2{}^{17}O$	$H_2{}^{18}O$
SN1	1159	2199
SN2	1528	2650
FSN	0	5
ORP	0	3
Sum	2687	4849

[a] SN: spectroscopic network, SN1: *para* transitions for the symmetrically substituted isotopologues, SN2: *ortho* transitions for the symmetrically substituted isotopologues, FSN: floating spectroscopic network (see text), ORP: orphan transitions (see text). For $H_2{}^{18}O$, the FSNs and ORPs were not included in the total sum as they could not be validated.

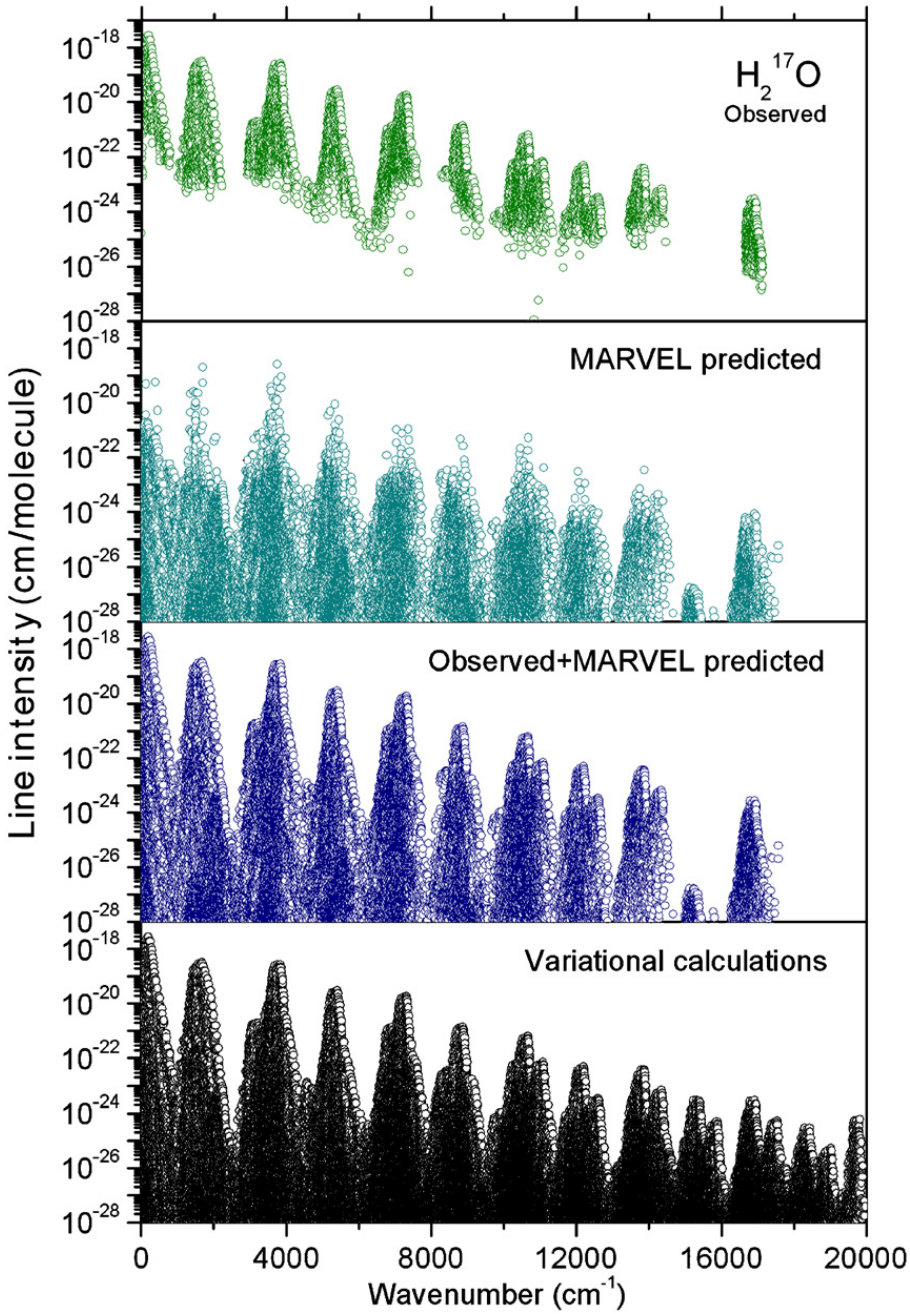

Fig. 2. Observed (top panel), MARVEL predicted (second panel), their sum (third panel) transitions based on predictions from the variational calculations of Shirin et al. [70] (bottom panel) for $H_2{}^{17}O$. Calculated line intensities are used in each case.

Author's personal copy

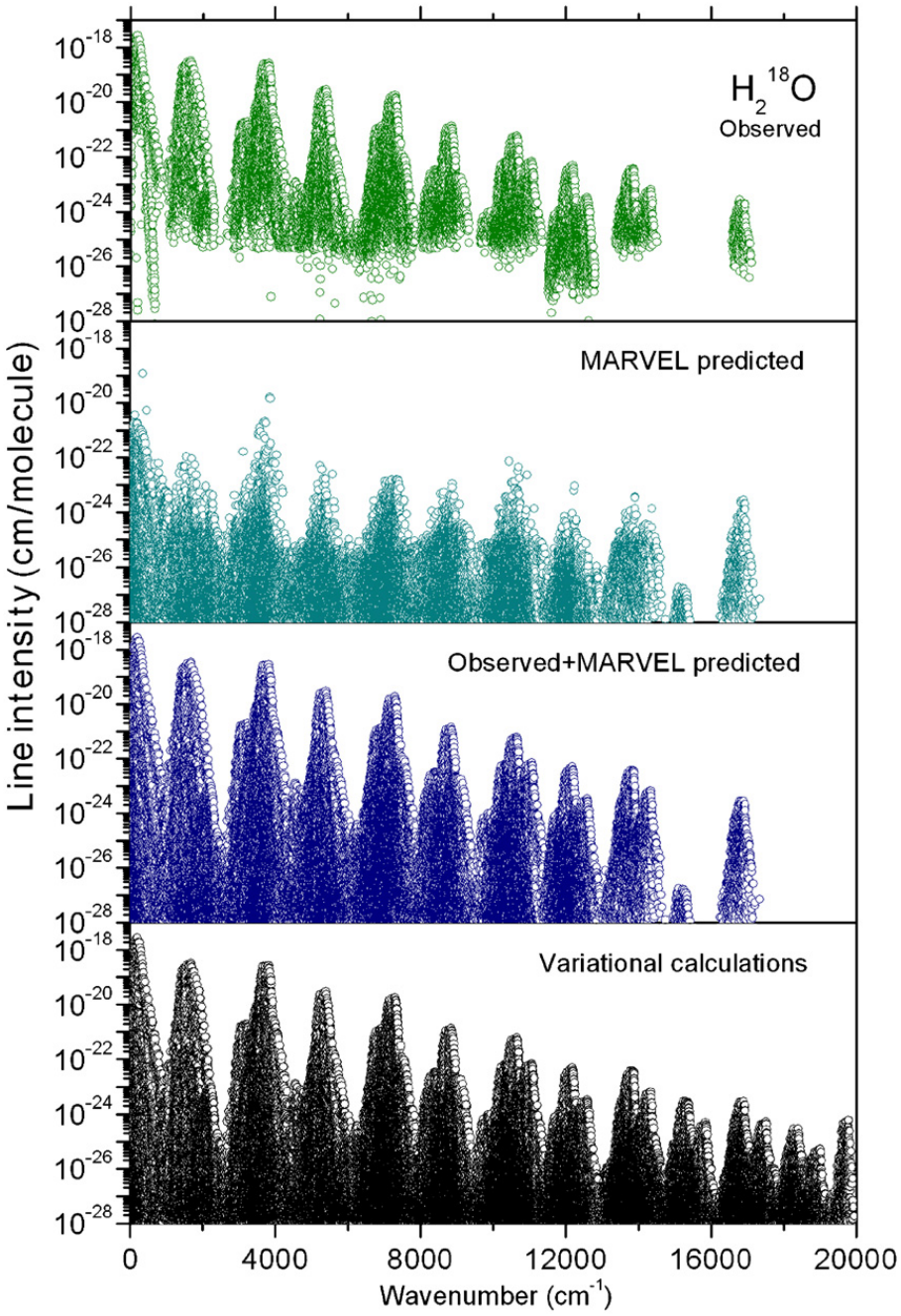

Fig. 3. Observed (top panel), MARVEL predicted (second panel), their sum (third panel) transitions based on predictions from the variational calculations of Shirin et al. [70] (bottom panel) for $H_2{}^{18}O$. Calculated line intensities are used in each case.

ideal platform to achieve the goal of determining accurate rovibrational energy levels from which precise line positions can be computed straightforwardly.

Precision of the energy levels determined in this study is dependent upon several factors. Most important among these is the precision of the observed transitions. An important related result of our analysis is that often the experimental uncertainties given in the original publications are overly optimistic, in a large number of cases the given experimental uncertainties had to be increased by at least a factor of 10 in order to obtain a self-consistent database. Since our analysis utilized all available experimental information, there are many energy levels which are involved in multiple transitions measured by different experimental groups utilizing different spectrometers and experimental conditions. We consider an energy level particularly well determined, i.e., precise, if it is involved in more than five transitions and there are at least two independent experimental investigations which relied on this energy level. These energy levels are graded as A+ in the Supplementary Material. This means that the value of the energy level, within the stated uncertainty, and its assignment are dependable and should be particularly useful in future studies and in modeling work. Those energy levels which are involved in more than five transitions but only in a single set of measurements received an A− grade. These levels should

Author's personal copy

be considered as precise values, again within their stated uncertainty, but independent verification of them is desirable. Energy levels which are involved in between two and five transitions and were subjected to one or more experimental investigations are grade B− and B+, respectively. The energy levels which were involved in just one measured transition are denoted as C and should not be considered as precisely determined levels and must only be employed with considerable care. The most important argument supporting inclusion of grade C levels in the final results of this study is that they have been verified by variational nuclear motion computations. Nevertheless, the stated uncertainties of these levels are probably overly optimistic as they come from a single source.

Over the course of the present study it became clear that determination of a precise set of energy levels requires not only dependable experimental data but also a first-principles approach to determine as accurate energy levels as possible. This was provided here by variational nuclear motion computations employing the most accurate empirical PESs of water, and an empirical approach, like MARVEL, which allows determination of sets of self-consistent levels and lines and their uncertainties.

For $H_2{}^{18}O$ our cleansed set includes 29 364 transitions that correspond to 17 034 entries with unique assignments, that, in turn, corresponds to, once multiple assignments to the same line are excluded, about 16 200 experimental lines. This set yielded 4849 MARVEL energy levels. One use of these energies is to generate high accuracy line positions for still unobserved transitions. We generated such list of transitions for $H_2{}^{18}O$; it contains 28 800 transitions with intensities from the variational calculations [70] between 10^{-19} and 4×10^{-28} cm molecule^{-1}. For $H_2{}^{17}O$, there is less experimental information: the final cleaned set consists of 8614 transitions that corresponds to 6772 unique assignments, and about 6500 spectral lines. These give 2687 energy levels. Using these energy levels give 20 825 lines in the same intensity window. This is a much more significant increase than for $H_2{}^{18}O$. Figs. 2 and 3 show these yet to be observed transitions for $H_2{}^{17}O$ and $H_2{}^{18}O$ respectively.

While for $H_2{}^{17}O$ it is clear that there are many regions for which laboratory data are missing, the coverage for $H_2{}^{18}O$ is reasonable up to 15 000 cm^{-1}. Above 15 000 cm^{-1}, however, there is only very limited data available. It is clear that at these higher frequencies there are some significant bands about which nothing is known experimentally at present.

Finally, we note that the present IUPAC TG effort has already proven valuable for the development of the next edition of HITRAN [4]. As mentioned above, the parameters in HITRAN are a mixture of experimentally and theoretically determined quantities. Furthermore, thespectral region covered is from 0 to over 25 000 cm^{-1} for H_2O (microwave through visible). Consequently, for almost all molecules contained in HITRAN, the data have come from different sources depending on the spectral region. There has not been an overly great effort in many cases to ensure that these data are consistent, although this issue has been receiving more attention recently. In the case of using the MARVEL program, there is indeed as much self-consistency as possible in the results. Already comparisons of these results have pointed to some errors in the linelists that were incorporated into HITRAN, and these will be corrected. More importantly, this work has provided impetus to update some of the older and less reliable data. It should also be mentioned that there has existed a high-temperature analog to HITRAN, namely HITEMP [127]. The original version contains linelists for H_2O, CO_2, CO, and OH. The line positions and intensities for water-vapor were based on a theoretical calculation [128] appropriate for 1000 K, with a supplemental limited linelist calculated for 1500 K. A new edition of HITEMP is now being prepared [129], based on a greatly improved theoretical calculation [123]. It is anticipated that the IUPAC TG's attention to high-temperature data will greatly influence this new database. In summary, the IUPAC approach and the database created form a paradigm for the further development of the HITRAN database.

Acknowledgments

We all thank the International Union of Pure and Applied Chemistry for funding under Project 2004-035-1-100 (A database of water transitions from experiment and theory). In addition, this work has received partial support from the UK Engineering and Physical Science Research Council, the UK Natural Environment Research Council, the Royal Society, the British Council, the INTAS foundation, Grant WWLC-008535-(reintegration) MCA FP6 EC, the Scientific Research Fund of Hungary (Grants OTKA T47185 and K72885), the NKTH, the European Union QUASAAR Marie Curie research training network, NATO, the Russian Foundation for Basic Research, the Belgian Federal Science Policy Office (Contracts EV/35/3A, SD/AT/01A, PRODEX 1514901NLSFe(IC)), the Belgian National Fund for Scientific Research (FRFC contracts), the Communauté de Belgique (Action de Recherche Concertées), NASA Earth Observing System (EOS), under the Grant NAG5-13534, the NASA laboratory astrophysics program. Alain Campargue and Ludovic Daumont are grateful for the financial support provided by the Programme National LEFE (CHAT) of CNRS (INSU). Part of the research described in this paper was performed at the Jet Propulsion Laboratory, California Institute of Technology, under contract with The National Aeronautics and Space Administration.

Appendix A. Supplementary data

Supplementary data associated with this article can be found in the online version at doi:10.1016/j.jqsrt.2009.02.014.

Author's personal copy

References

[1] Polyansky OL. One-dimensional approximation to the effective rotational Hamiltonian of the ground-state of the water molecule. J Mol Spectrosc 1985;112:79–87.
[2] Bernath PF. The spectroscopy of water vapour: experiment, theory and applications. Phys Chem Chem Phys 2002;4:1501–9.
[3] Rothman LS, Jacquemart D, Barbe A, Benner DC, Birk M, Brown LR, et al. The HITRAN 2004 molecular spectroscopic database. JQSRT 2005;96:139–204.
[4] Rothman LS, Gordon IE, Barbe A, Benner DC, Bernath PF, Birk M, et al. The *HITRAN* 2008 molecular spectroscopic database. JQSRT 2009, this issue. doi:10.1016/j.jqsrt.2009.02.013.
[5] Tolchenov R, Tennyson J. Water line parameters from refitted spectra constrained by empirical upper state levels: study of the 9500−14 500 cm^{-1} region. JQSRT 2008;109:559–68.
[6] Vidler M, Tennyson J. Accurate partition function and thermodynamic data for water. J Chem Phys 2000;113:9766–71.
[7] Gates DM, Calfee RF, Hansen DW, Benedict WS. Line parameters and computed spectra for water vapor bands at 2.7 μm. Natl Bur Stand Monogr 1964;71.
[8] Flaud J-M, Camy-Peyret C, Toth RA. Water vapour line parameters from microwave to medium infrared. Oxford: Pergamon Press; 1981.
[9] Tennyson J, Zobov NF, Williamson R, Polyansky OL, Bernath PF. Experimental energy levels of the water molecule. J Phys Chem Ref Data 2001;30:735–831.
[10] Furtenbacher T, Császár A, Tennyson J. MARVEL: measured active rotational–vibrational energy levels. J Mol Spectrosc 2007;245:115–25.
[11] Császár AG, Czakó G, Furtenbacher T, Mátyus E. An active database approach to complete spectra of small molecules. Ann Rep Comput Chem 2007;3:155–76.
[12] Furtenbacher T, Császár AG. On employing $H_2{}^{16}O$, $H_2{}^{17}O$, $H_2{}^{18}O$, and $D_2{}^{16}O$ lines as frequency standards in the 15−170 cm^{-1} window. JQSRT 2008;109:1234–51.
[13] Bykov AD, Fazliev AZ, Filippov NN, Kozodoev AV, Privezentsev AI, Sinitsa LN, et al. Distributed information system on atmospheric spectroscopy. Geophys Res Abstr 2007;9:01906 [SRef-ID: 1607-7962/gra/EGU2007-A-01906].
[14] Császár AG, Fazliev AZ, Tennyson J. W@DIS—prototype information system for systematization of spectral data of water. In: Abstracts of the twentieth colloquium on high resolution molecular spectroscopy, Dijon, France, 2007.
[15] Flaud J-M, Camy-Peyret C, Maillard JP. Higher ro-vibrational levels of H_2O deduced from high-resolution oxygen–hydrogen flame spectra between 2800−6200 cm^{-1}. Mol Phys 1976;32:499–521.
[16] Ruscic B, Pinzon RE, Morton ML, Von Laszevski G, Bittner SJ, Nijsure SG, et al. Introduction to active thermochemical tables: several "key" enthalpies of formation revisited. J Phys Chem A 2004;108:9979–97.
[17] Watson JKG. Robust weighting in least-squares fits. J Mol Spectrosc 2003;219:326–8.
[18] Miani A, Tennyson J. Can ortho–para transitions for water be observed? J Chem Phys 2004;120:2732–9.
[19] Fraley PE, Narahari Rao K, Jones LH. High resolution infrared spectra of water vapor. ν_1 and ν_3 bands of $H_2{}^{18}O$. J Mol Spectrosc 1969;29:312–47.
[20] Hindman JC, Zielen AJ, Svirmickas A, Wood M. Relaxation processes in water. The spin-lattice relaxation of the deuteron in D_2O and oxygen-17 in $H_2{}^{17}O$. J Chem Phys 1971;54:621–34.
[21] Steenbeckeliers G, Bellet J. Spectre micro-onde des molćules $H_2{}^{16}O$, $H_2{}^{17}O$ et $H_2{}^{18}O$. C R Acad Sci Ser B 1971;273:471–4.
[22] Williamson JG, Narahari Rao K, Jones LH. High-resolution infrared spectra of water vapor ν_2 band of $H_2{}^{18}O$. J Mol Spectrosc 1971;40:372–87.
[23] DeLucia FC, Helminger P, Cook RL, Gordy W. Submillimetrer microwave spectrum of $H_2{}^{16}O$. Phys Rev A 1972;5:487–90.
[24] DeLucia FC, Gordy W, Cook RL, Helminger P. Submillimetrer microwave spectrum of $H_2{}^{18}O$. Phys Rev A 1972;6:1324–6.
[25] Camy–Peyret C, Flaud J-M, Guelachvili G, Amiot C. High resolution Fourier transform spectrum of water between 2930 and 4255 cm^{-1}. Mol Phys 1973;26:825–55.
[26] DeLucia FC, Helminger P, Kirchhoff WH. Microwave spectra of molecules of astrophysical interest V. Water vapor. J Phys Chem Ref Data 1974;3:211–9.
[27] DeLucia FC, Helminger P. Microwave spectrum and ground state energy levels of $H_2{}^{17}O$. J Mol Spectrosc 1975;56:138–45.
[28] Winther F. The rotational spectrum of water between 650 and 50 cm^{-1}. J Mol Spectrosc 1977;65:405–19.
[29] Toth RA, Flaud J-M, Camy-Peyret C. Spectrum of $H_2{}^{18}O$ and $H_2{}^{17}O$ in the 5030 to 5640 cm^{-1} region. J Mol Spectrosc 1977;67:185–205.
[30] Toth RA, Flaud J-M, Camy–Peyret C. Spectrum of $H_2{}^{18}O$ and $H_2{}^{17}O$ in the 6974 to 7387 cm^{-1} region. J Mol Spectrosc 1977;67:206–18.
[31] Lovas FJ. Microwave spectral tables. II. Triatomic molecules. J Phys Chem Ref Data 1978;7:1445–750.
[32] Helminger P, De Lucia FC. Centrifugal distortion analysis of the ground vibrational states of $H_2{}^{17}O$ and $H_2{}^{18}O$. J Mol Spectrosc 1978;70:263–9.
[33] Kauppinen J, Käkkäinen T, Kyrö E. High-resolution spectrum of water vapor between 30 and 720 cm^{-1}. J Mol Spectrosc 1978;71:15–45.
[34] Johns JWC, McKellar ARW. Stark Spectroscopy with the CO Laser: Lamb bip Spectra of $H_2{}^{17}O$ and $H_2{}^{18}O$ in the ν_2 fundamental band. Can J Phys 1978;56:737–43.
[35] Kauppinen J, Kyrö E. High resolution pure rotational spectrum of water vapor enriched by $H_2{}^{17}O$ and $H_2{}^{18}O$. J Mol Spectrosc 1980;84:405–23.
[36] Camy-Peyret C, Flaud J-M, Papineau N. La bande ν_2 des espéces isotopiques $H_2{}^{17}O$ et $H_2{}^{18}O$. C R Acad Sci Paris Ser B 1980;290:537–40.
[37] Kyrö E. Centrifugal distortion analysis of pure rotational spectra of $H_2{}^{16}O$, $H_2{}^{17}O$, and $H_2{}^{18}O$. J Mol Spectrosc 1981;88:167–74.
[38] Partridge RH. Far-infrared absorption spectra of $H_2{}^{16}O$, $H_2{}^{17}O$, and $H_2{}^{18}O$. J Mol Spectrosc 1981;87:429–37.
[39] Camy-Peyret C, Flaud J-M, Toth RA. Line positions and intensities for the $2\nu_2$, ν_1 and ν_3 bands of $H_2{}^{17}O$. Mol Phys 1981;42:595–604.
[40] Toth RA. SISAM database ⟨http://mark4sun.jpl.nasa.gov/h2o.html⟩; 2007.
[41] Pine AS, Coulombe MJ, Camy-Peyret C, Flaud J-M. Atlas of the high-temperature water vapor spectrum in the 3000 to 4000 cm^{-1} region. J Phys Chem Ref Data 1983;12:413–65.
[42] Guelachvili G. Experimental Doppler-limited spectra of the ν_2-bands of $H_2{}^{16}O$, $H_2{}^{17}O$, $H_2{}^{18}O$, and HDO by Fourier-transform spectroscopy: secondary wave-number standards between 1066 and 2296 cm^{-1}. J Opt Soc Am 1983;73:137–50.
[43] Bykov AD, Saveliev VN, Ulenikov ON. Rotational and centrifugal parameters of $H_2{}^{17}O$ and $H_2{}^{18}O$ (0 1 0) states. J Mol Spectrosc 1986;118:313–5.
[44] Toth RA. Transition frequencies and absolute strengths of $H_2{}^{17}O$ and $H_2{}^{18}O$ in the 6.2 – μm region. J Opt Soc Am B 1992;9:462–82.
[45] Toth RA. $2\nu_2$–ν_2 and $2\nu_2$ bands of $H_2{}^{16}O$, $H_2{}^{17}O$, and $H_2{}^{18}O$: line positions and strengths. J Opt Soc Am B 1993;10:1526–44.
[46] Toth RA. The ν_1 and ν_3 bands of $H_2{}^{17}O$ and $H_2{}^{18}O$: line positions and strengths. J Mol Spectrosc 1994;166:184–203.
[47] Toth RA. Transition frequencies and strengths of $H_2{}^{17}O$ and $H_2{}^{18}O$: 6600 to 7640 cm^{-1}. Appl Opt 1994;33:4868–79.
[48] Vaara J, Lounila J, Ruud K, Helgaker T. Rovibrational effects, temperature dependence, and isotope effects on the nuclear shielding tensor of water: a new ^{17}O absolute shielding scale. J Chem Phys 1998;109:8388–97.
[49] Toth RA. Water vapor measurements between 590 and 2582 cm^{-1}: line positions and strengths. J Mol Spectrosc 1998;190:379–96.
[50] Matsushima F, Nagase H, Nakauchi T, Odashima H, Takagi K. Frequency measurement of pure rotational transitions of $H_2{}^{17}O$ and $H_2{}^{18}O$ from 0.5 to 5 THz. J Mol Spectrosc 1999;193:217–23.
[51] Camy-Peyret C, Flaud J-M, Mandin J-Y, Bykov A, Naumenko O, Sinitsa L, et al. Fourier-transform absorption spectrum of the $H_2{}^{17}O$ molecule in the 9711−11 335 cm^{-1} spectral region: the first decade of resonating states. JQSRT 1999;61:795–812.
[52] Kerstel ERT, Gagliardi G, Gianfrani L, Meijer HAJ, van Trigt R, Ramaker R. Determination of the $^2H/^1H$, $^{17}O/^{16}O$, and $^{18}O/^{16}O$ isotope ratios in water by means of tunable diode laser spectroscopy at 1.39 μm. Spectrochim Acta Part A 2002;58:2389–96.
[53] Mikhailenko SN, Tyuterev VG, Starikov VI, Albert KK, Winnewisser BP, Winnewisser M, et al. Water Spectra in the region 4200–6250 cm^{-1}; extended analysis of $\nu_1+\nu_2$, $\nu_2+\nu_3$, and $3\nu_2$ bands and confirmation of highly excited states from flame spectra and from atmospheric long-path observations. J Mol Spectrosc 2002;213:91–121.

Author's personal copy

[54] Gamache RR, Fischer J. Half-widths of $H_2{}^{16}O$, $H_2{}^{18}O$, $H_2{}^{17}O$, $HD^{16}O$, and $D_2{}^{16}O$ I. Comparison between isotopomers. JQSRT 2003;78:289–304.
[55] Gamache RR, Fischer J. Half-widths of $H_2{}^{16}O$, $H_2{}^{18}O$, $H_2{}^{17}O$, $HD^{16}O$, and $D_2{}^{16}O$: II. Comparison with measurement. JQSRT 2003;78:305–18.
[56] Lemus R. Vibrational excitations in H_2O in the framework of a local model. J Mol Spectrosc 2004;225:73–92.
[57] Macko P, Romanini D, Mikhailenko SN, Naumenko OV, Kassi S, Jenouvrier A, et al. High sensitivity CW-cavity ring down spectroscopy of water in the region of the 1.5 μm atmospheric window. J Mol Spectrosc 2004;227:90–108.
[58] Toth RA. Measurements and analysis (using empirical functions for widths) of air- and self-broadening parameters of H_2O. JQSRT 2005;94:1–50.
[59] Toth RA. Measurements of positions, strengths and self-broadened widths of H_2O from 2900 to 8000 cm^{-1}: line strength analysis of the 2nd triad bands. JQSRT 2005;94:51–107.
[60] Tolchenov RN, Tennyson J. Water line parameters for weak lines in the range 7400−9600 cm^{-1}. J Mol Spectrosc 2005;231:23–7.
[61] Tanaka M, Naumenko O, Brault JW, Tennyson J. Fourier transform absorption spectra of $H_2{}^{18}O$ and $H_2{}^{17}O$ in the $3\nu+\delta$ and 4ν polyad region. J Mol Spectrosc 2005;234:1–9.
[62] Franz P, Röckmann T. High-precision isotope measurements of $H_2{}^{16}O$, $H_2{}^{17}O$ and $H_2{}^{18}O$, and the $\Delta^{17}O$-anomaly of water vapor in the southern lowermost stratosphere. Atmos Chem Phys 2005;5:2949–59.
[63] Tolchenov RN, Naumenko O, Zobov NF, Shirin SV, Polyansky OL, Tennyson J, et al. Water vapor line assignments in the 9250−26 000 cm^{-1} frequency range. J Mol Spectrosc 2005;233:68–76.
[64] Liu A-W, Hu S-M, Camy-Peyret C, Mandin J-Y, Naumenko O, Voronin B. Fourier transform absorption spectra of $H_2{}^{17}O$ and $H_2{}^{18}O$ in the 8000−9400 cm^{-1} spectral region. J Mol Spectrosc 2006;237:53–62.
[65] Naumenko O, Sneep M, Tanaka M, Shirin SV, Ubachs W, Tennyson J. Cavity ring-down spectroscopy of $H_2{}^{17}O$ in the range 16 570−17 125 cm^{-1}. J Mol Spectrosc 2006;237:63–9.
[66] Mazzotti F, Tolchenov RN, Campargue A. High sensitivity ICLAS of $H_2{}^{18}O$ in the region of the second decade (11 520−12 810 cm^{-1}). J Mol Spectrosc 2007;243:78–89.
[67] Jenouvrier A, Daumont L, Régalia–Jarlot L, Tyuterev VG, Carleer M, Vandaele AC, et al. Fourier transform measurements of water vapor line parameters in the 4200−6600 cm^{-1} region. JQSRT 2007;105:326–55.
[68] Mikhailenko SN, Le W, Kassi S, Campargue A. Weak water absorption lines around 1.455 and 1.66 μm by CW-CRDS. J Mol Spectrosc 2007;244:170–8.
[69] Lisak D, Hodges JT. Low-uncertainty H_2O line intensities for the 930-nm region. J Mol Spectrosc 2008;249:6–13.
[70] Shirin SV, Ovsyannikov RI, Zobov NF, Polyansky OL, Tennyson J. Water line lists close to experimental accuracy using a spectroscopically determined potential energy surfaces for $H_2{}^{16}O$, $H_2{}^{17}O$ and $H_2{}^{18}O$. J Chem Phys 2008;128 [Article no. 224306].
[71] Jain SC, Bhandari RC. Some relaxational parameters of $H_2{}^{18}O$ and $D_2^{18}O$. J Chem Phys 1967;47:4867–9.
[72] Benedict WS, Pollack MA, Tomlinson III WJ. The water–vapor laser. IEEE J Quant Electron 1969;QE-5:108–24.
[73] Powell FX, Johnson DR. Microwave detection of $H_2{}^{18}O$. Phys Rev Lett 1970;24:637.
[74] Ball JA, Gottlieb CA, Radford HE. Search for extraterrestrial $H_2{}^{18}O$ emission. Astrophys J 1971;163:429–30.
[75] Toth RA, Margolis JS. Spectrum of $H_2{}^{18}O$ in 2900 to 3400 cm^{-1} region. J Mol Spectrosc 1975;57:236–45.
[76] Fleming JW, Gibson MJ. Far-infrared absorption spectra of water vapor $H_2{}^{16}O$ and isotopic modifications. J Mol Spectrosc 1976;62:326–37.
[77] Flaud J-M, Camy-Peyret C, Toth RA. The ground state (0 0 0) and the interacting states (1 1 0) and (0 1 1) of $H_2{}^{18}O$. J Mol Spectrosc 1977;68:280–7.
[78] Camy–Peyret C, Flaud J-M, Mandin J-Y, Toth RA. Line positions and intensities for $\nu_1+\nu_2$ and $\nu_2+\nu_3$ bands of $H_2{}^{18}O$. J Mol Spectrosc 1978;70:361–73.
[79] Flaud J-M, Camy–Peyret C, Toth RA. Line positions and intensities for the $2\nu_2$, ν_1, and ν_3 bands of $H_2{}^{18}O$. Can J Phys 1980;58:1748–57.
[80] Camy–Peyret C, Flaud J-M, Toth RA. The interacting states (0 2 0), (1 0 0), and (0 0 1) of $H_2{}^{17}O$ and $H_2{}^{18}O$. J Mol Spectrosc 1981;87:233–41.
[81] Toth RA, Brault JW. Line positions and strengths in the (0 0 1), (1 1 0), and (0 3 0) bands of HDO. Appl Opt 1983;22:908–26.
[82] Johns JWC. High-resolution far-infrared (20−350-cm^{-1}) spectra of several isotopic species of H_2O. J Opt Soc Am B 1985;2:1340–54.
[83] Chevillard J-P, Mandin J-Y, Flaud J-M, Camy-Peyret C. $H_2{}^{18}O$: the (0 3 0), (1 1 0), and (0 1 1) interacting states. Line positions and intensities $3\nu_2$, $\nu_1+\nu_2$, and $\nu_2+\nu_3$ bands. Can J Phys 1985;63:1112–27.
[84] Chevillard J-P, Mandin J-Y, Flaud J-M, Camy-Peyret C. The $2\nu_2+\nu_3-\nu_2$ hot band of $H_2{}^{18}O$ between 4800 and 6000 cm^{-1}: line positions and intensities. JQSRT 1986;36:395–9.
[85] Chevillard J-P, Mandin J-Y, Camy-Peyret C, Flaud J-M. The first hexad [(0 4 0), (1 2 0), (0 2 1), (2 0 0), (1 0 1), (0 0 2)] of $H_2{}^{18}O$: experimental energy levels and line intensities. Can J Phys 1986;64:746–61.
[86] Devi VM, Benner DC, Rinsland CP, Smith MAH, Sidney BD. Diode laser measurements of air and nitrogen broadening in the ν_2 bands of HDO, $H_2{}^{16}O$, and $H_2{}^{18}O$. J Mol Spectrosc 1986;117:403–7.
[87] Chevillard J-P, Mandin J-Y, Flaud J-M, Camy-Peyret C. $H_2{}^{18}O$: line positions and intensities between 9500 and 11 500 cm^{-1}. The (0 4 1), (2 2 0), (1 2 1), (3 0 0), (2 0 1), (1 0 2) and (0 0 3) interacting states. Can J Phys 1987;65:777–89.
[88] Belov SP, Kozin IN, Polyansky OL, Tretyakov MY, Zobov NF. Measurement and analysis of precise data using rotational and vibronic spectra of a water molecule: ground and 010 states of $H_2{}^{18}O$. Opt Spektrosk 1987;62:1244–8.
[89] Jensen P. The potential energy surface for the electronic ground state of the water molecule determined from experimental data using a variational approach. J Mol Spectrosc 1989;133:438–60.
[90] Ulenikov ON, Zhilyakov AS. Calculation of the $H_2{}^{18}O$ rotational energy levels for the first hexad of interacting vibrational states. J Mol Spectrosc 1989;133:1–9.
[91] Ulenikov ON, Zhilyakov AS. The line intensities of the $H_2{}^{18}O$ molecule first hexad interacting vibrational states. J Mol Spectrosc 1989;133:239–43.
[92] Ulenikov ON, Zhilyakov AS, Shevchenko GA. The line intensities of the $2\nu_2+\nu_3-\nu_2$ hot band of $H_2{}^{18}O$. J Mol Spectrosc 1989;133:224–6.
[93] Makushkin YS, Ulenikov ON, Levashkin IV. Energy spectrum and spectroscopic parameters of the first decade of the $H_2{}^{18}O$ molecule. J Mol Spectrosc 1990;144:1–17.
[94] Makushkin YS, Ulenikov ON, Zhilyakov AS. Transformed dipole moment and line intensities for the $H_2{}^{18}O$ molecule first decade interacting vibrational states. J Mol Spectrosc 1990;144:239–41.
[95] Sasada H, Takeuchi S, Iritani M, Nakatani K. Semiconductor-laser heterodyne frequency measurements of 1.52 μm molecular transitions. J Opt Soc Am B 1991;8:713–8.
[96] Rinsland CP, Smith MAH, Devi VM, Benner DC. Measurements of Lorentz-broadening coefficients and pressure-induced line shift coefficients in the ν_2 band of $HD^{16}O$. J Mol Spectrosc 1991;150:640–6.
[97] Rinsland CP, Smith MAH, Devi VM, Benner DC. Measurement of Lorentz-broadening coefficients and pressure-induced line-shift coefficients in the ν_1 band of $HD^{16}O$ and the ν_3 band of $D_2{}^{16}O$. J Mol Spectrosc 1992;156:507–11.
[98] Bykov A, Naumenko O, Petrova T, Scherbakov A, Sinitsa L, Mandin J-Y, et al. The second decade of $H_2{}^{18}O$: line positions and energy levels. J Mol Spectrosc 1995;172:243–53.
[99] Toth RA, Brown LR, Plymate C. Self-broadened widths and frequency shifts of water vapor lines between 590 and 2400 cm^{-1}. JQSRT 1998; 59:529–62.
[100] Toth RA. Air- and N_2-broadening parameters of water vapor: 604 to 2271 cm^{-1}. J Mol Spectrosc 2000;201:218–43.
[101] Gagliardi G, Rusciano G, Gianfrani L. Sub-Doppler spectroscopy of $H_2{}^{18}O$ at 1.5 μm. Appl Phys B 2000;70:883–8.
[102] Moretti L, Sasso A, Gianfrani L, Ciurylo R. Collision-broadened and Dicke-narrowed lineshapes of $H_2{}^{16}O$ and $H_2{}^{18}O$ transitions at 1.39 μm. J Mol Spectrosc 2001;205:20–7.
[103] Tanaka M, Brault JW, Tennyson J. Absorption spectrum of $H_2{}^{18}O$ in the range 12 400–14 520 cm^{-1}. J Mol Spectrosc 2002;216:77–80.
[104] Mikhailenko SN, Tyuterev VG, Mellau G. (0 0 0) and (0 1 0) states of $H_2{}^{18}O$: analysis of rotational transitions in hot emission spectrum in the 400−850 cm^{-1} region. J Mol Spectrosc 2003;217:195–211.

Author's personal copy

[105] Tanaka M, Sneep M, Ubachs W, Tennyson J. Cavity ring-down spectroscopy of $H_2{}^{18}O$ in the range 16 570−17 120 cm^{-1}. J Mol Spectrosc 2004;226:1–26.
[106] Liu A-W, Naumenko O, Song K-F, Voronin BA, Hu S-M. Fourier-transform absorption spectroscopy of $H_2{}^{18}O$ in the first hexade region. J Mol Spectrosc 2006;236:127–33.
[107] Golubiatnikov GY, Markov VN, Guarnieri A, Knöchel R. Hyperfine structure of $H_2{}^{16}O$ and $H_2{}^{18}O$ measured by Lamb-dip technique in the 180–560 GHz frequency range. J Mol Spectrosc 2006;240:191–4.
[108] Liu A-W, Du J-H, Song K-F, Wang L, Wan L, Hu S-M. High-resolution Fourier-transform spectroscopy of ^{18}O-enriched water molecule in the 1080−7800 cm^{-1} region. J Mol Spectrosc 2006;237:149–62.
[109] Joly L, Parvitte B, Zéninari V, Courtois D, Durry G. A spectroscopic study of water vapor isotopologues $H_2{}^{16}O$, $H_2{}^{18}O$ and HDO using a continuous wave DFB quantum cascade laser in the 6.7 μm region for atmospheric applications. JQSRT 2006;102:129–38.
[110] Shirin SV, Polyansky OL, Zobov NF, Ovsyannikov RI, Császár AG, Tennyson J. Spectroscopically determined potential energy surfaces of the $H_2{}^{16}O$, $H_2{}^{17}O$ and $H_2{}^{18}O$ isotopologues of water. J Mol Spectrosc 2006;236:216–23.
[111] Polyansky OL, Császár AG, Shirin SV, Zobov NF, Barletta P, Tennyson J, et al. High accuracy ab initio rotation–vibration transitions of water. Science 2003;299:539–42.
[112] Barletta P, Shirin SV, Zobov NF, Polyansky OL, Tennyson J, Valeev EF, et al. CVRQD ab initio adiabatic ground-state potential surfaces for the water molecule. J Chem Phys 2006;125 [Article no. 204307].
[113] Guelachvili G, Birk M, Bordé CJ, Brault JW, Brown LR, Carli B, et al. High resolution wavenumber standards for the infrared. J Mol Spectrosc 1996;177:164–79.
[114] Voronin BA, Naumenko OV, Carleer M, Coheur P-F, Fally S, Jenouvrier A, et al. HDO absorption spectrum above 11 500 cm^{-1}: assignment and dynamics. J Mol Spectrosc 2007;244:87–101.
[115] Schermaul R, Learner RCM, Canas AAD, Brault JW, Polyansky OL, Belmiloud D, et al. Weak line water vapor spectrum in the regions 13 200−15 000 cm^{-1}. J Mol Spectrosc 2002;211:169–78.
[116] Tennyson J, Kostin MA, Barletta P, Harris GJ, Polyansky OL, Ramanlal J, et al. DVR3D: a program suite for the calculation of rotation–vibration spectra of triatomic molecules. Comput Phys Commun 2004;163:85–116.
[117] Polyansky OL, Zobov NF, Viti S, Tennyson J, Bernath PF, Wallace L. K-band spectrum of water in sunspots. Astrophys J 1997;489:L205–8.
[118] Zobov NF, Ovsyannikov RI, Shirin SV, Polyansky OL. The assignment of quantum numbers in the theoretical spectra of the $H_2{}^{16}O$, $H_2{}^{17}O$ and $H_2{}^{18}O$ molecules calculated by variational methods in the region 0–26 000 cm^{-1}. Opt Spectrosc 2007;102:348–53.
[119] Child MS, Halonen L. Overtone frequencies and intensities in the local mode picture. Adv Chem Phys 1984;57:1–58.
[120] Carleer M, Jenouvrier A, Vandaele A-C, Bernath PF, Mérienne MF, Colin R, et al. The near infrared, visible and near ultraviolet overtone spectrum of water. J Chem Phys 1999;111:2444–50.
[121] Császár AG, Allen WD, Yamaguchi Y, Schaefer HF. Ab initio determination of accurate ground electronic state potential energy hypersurfaces for small molecules. In: Computational molecular spectroscopy. New York: Wiley; 2000. p. 15–68.
[122] Császár AG, Tarczay G, Leininger ML, Polyansky OL, Tennyson J, Allen WD. Dream or reality: complete basis set full configuration interaction potential energy hypersurfaces. In: Spectroscopy from space. Dordrecht: Kluwer; 2001. p. 317–39.
[123] Barber RJ, Tennyson J, Harris GJ, Tolchenov RN. A high accuracy computed water line list. Mon Not R Astron Soc 2006;368:1087–94.
[124] Jacquemart D, Gamache R, Rothman LS. Semi-empirical calculation of air-broadened half-widths and air pressure-induced frequency shifts of water-vapor absorption lines. JQSRT 2005;96:205–39.
[125] Kozin IN, Pavlichenkov IM. Bifurcation in rotational spectra of nonlinear AB_2 molecules. J Chem Phys 1996;104:4105–13.
[126] Jucks K. private communication, 2003.
[127] Rothman LS, Wattson RB, Gamache RR, Schroeder J, McCann A. HITRAN, HAWKS and HITEMP high-temperature molecular database. In: Proceedings of the society of photo optical instrumentation engineers, vol. 2471, 1995. p. 105–11.
[128] Wattson RB, Rothman LS. Direct numerical diagonalization: wave of the future. JQSRT 1992;48:763–80.
[129] Rothman LS, Gordon IE, Barber RJ, Dothe H, Goldman A, Perevalov V, et al. HITEMP, the high-temperature molecular spectroscopic database. JQSRT 2009, in preparation.